

Area 3a: Topographic Organization and Cortical Connections in Marmoset Monkeys

Kelly J. Huffman and Leah Krubitzer

Center for Neuroscience and Department of Psychology,
University of California, Davis, Davis, CA 95616, USA

The functional organization of area 3a, a cortical field proposed to be involved in somato-motor-vestibular integration, has never been described for any primate. In the present investigation, the topographic organization and connections of area 3a were examined in marmosets using electrophysiological recording and anatomical tracing techniques. Multi-unit neuronal activity was recorded at a number of closely spaced sites; receptive fields (RFs) for neurons were determined, and the optimal stimulus was identified. In all cases, neurons in area 3a responded to the stimulation of deep receptors on the contralateral body. The representation of the body in area 3a was from the toes and foot, to the hindlimb, trunk, forelimb, hand and face in a mediolateral progression. In all cases electrophysiological results were related to myeloarchitecture, and the map in area 3a was found to be coextensive with a strip of lightly to moderately myelinated cortex just rostral to the darkly myelinated 3b. To examine the cortical connections of area 3a, injections of anatomical tracers were made into electrophysiologically identified body part representations. Area 3a has dense intrinsic connections and receives substantial inputs from the primary motor cortex (M1), the supplementary motor area (SMA), areas 1 and 2, the second somatosensory area (S2), and areas in posterior parietal cortex (PP). The connections of area 3a indicate that integration of cortical representations of body parts occurs both within area 3a and between area 3a and other somatosensory and motor areas. In addition, there are differential patterns of interconnections between behaviorally relevant body part representations of area 3a, such as the forelimb, compared to other body part representations (hindlimb/trunk), especially with 'higher order' cortical fields. This suggests that 3a may be an important component in a network that generates a common frame of reference for hand and eye coordinated reaching tasks.

Introduction

Primates use their hands with extraordinary precision to manipulate objects. The motor aspect of a simple manipulation task requires the coordinated activity of the digits, wrists, and forelimbs, usually on both sides of the body. The somatosensory system must supply the motor cortex and other related sub-cortical structures with relevant information regarding the position of the limbs in space, muscle load and tension, and the location of stimulus contact at different points across the hand. The somatosensory system must also provide the motor cortex with feedback regarding changes in position and stimulation patterns across the hand. This input to the motor system is critical for the initiation and continuation of the movements necessary for object manipulation.

Area 3a, which has been implicated in this process in primates, receives input from muscle spindles, which code muscle stretch information (Oscarsson and Rosén, 1966; Landgren and Silfvenius, 1969; Phillips *et al.*, 1971; Schwarz *et al.*, 1973; Lucier *et al.*, 1975; Heath *et al.*, 1976; Hore *et al.*, 1976; Zarzecki *et al.*, 1978; Wiesendanger and Miles, 1982) [see Jones and

Porter for a review (Jones and Porter, 1980)]. Although some characteristics of single neurons in area 3a have been examined, and partial connection patterns have been described, no study has provided a complete somatotopic representation (map), or described the full complement of ipsilateral and callosal cortical connections in any primate. A complete map of area 3a has been described in the flying fox (Krubitzer *et al.*, 1998). However, the flying fox has a highly derived hand (the wing) that is not used for object manipulation.

The lack of information on the organization and connections of area 3a in primates is due, in part, to its location. In macaque monkeys, area 3a is difficult to access with a recording electrode; the area lies on the fundus and deep in the rostral and/or caudal bank of the central sulcus. Even a number of commonly used New World monkeys such as the squirrel monkey and cebus monkey have a central sulcus or a central dimple (owl monkeys) in which area 3a resides. Thus, our choice of primate, the common marmoset (*Callithrix jacchus*), was guided primarily by the nearly lissencephalic nature of its cortex. In this species area 3a lies on the cortical surface and its location is optimal for obtaining detailed maps, and for the placement of injections (Fig. 1a). Another advantage of using marmoset monkeys is their position in primate evolution. Although these monkeys are highly specialized in many ways, marmosets are considered among the most primitive of simian primates (Beattie, 1927), and therefore may have basic cortical field characteristics that have been retained throughout primate evolution (Krubitzer and Kaas, 1990a). Finally, a number of other regions of somatosensory (Carlson *et al.*, 1986; Krubitzer and Kaas, 1990a, 1992), visual (Krubitzer and Kaas, 1990b, 1993; Fritsches and Rosa, 1996; Rosa *et al.*, 1997) and auditory cortex (Aitkin *et al.*, 1986, 1988; Luethke *et al.*, 1989; Aitkin and Park, 1993) have already been described using electrophysiological, neuroanatomical and architectonic techniques (Fig. 1a). Thus, assignment of fields that provide input to area 3a can be done with accuracy.

In the current study, we used multi-unit electrophysiological recording and anatomical tracing techniques to determine the detailed topographic organization and connections of area 3a in the marmoset monkey. Cortical maps generated from this study were related to patterns of myeloarchitecture determined from tangentially sectioned tissue. Both cortical organization and myeloarchitecture were related to connections from electrophysiologically identified locations in area 3a.

Materials and Methods

Multi-unit microelectrode recording techniques were used to identify the location, boundaries and topographic organization of somatosensory area 3a, or to guide injection placement in eight adult marmoset monkeys (*Callithrix jacchus*). Full or partial maps were made in six animals, and four injections were made in three animals. In all cases, cortices were flattened, cut parallel to the surface, and stained for myelin. Myeloarchitectonic boundaries were related to the electrophysiological

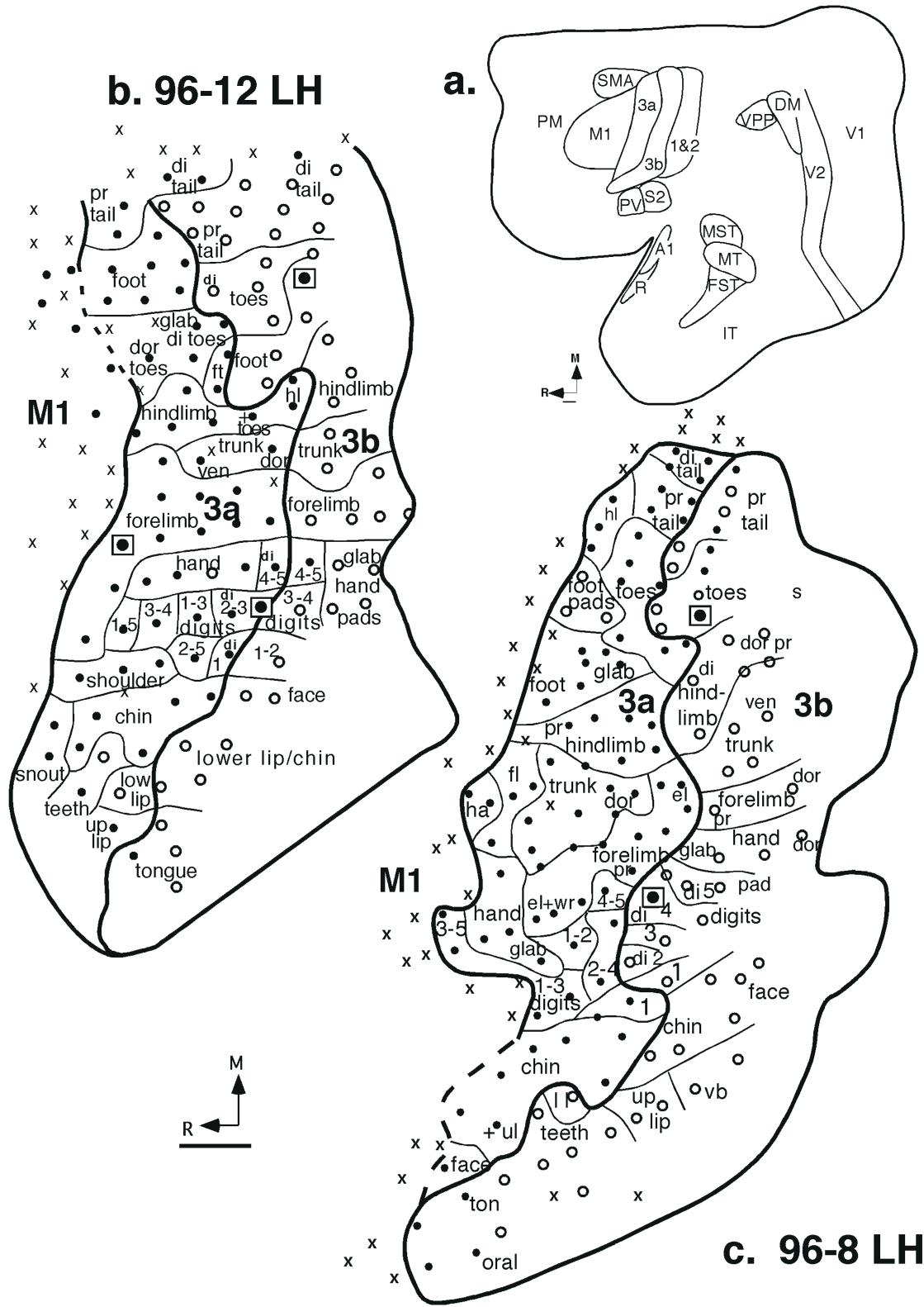


Figure 1. (a) A reconstructed flattened left hemisphere in the marmoset monkey. The lateral sulcus has been opened, and the medial wall retracted. The boundaries of cortical fields were drawn from an entire series of sections stained for myelin, and then collapsed onto one drawing. A map of area 3a, and neighboring cortex in the flattened left hemisphere of cases 96-12 (b) and 96-8 (c). Area 3a is organized topographically with the tail represented most medially, followed by the representations of the foot, toes, hindlimb and trunk. More laterally located are the representations of the hand, digits and face. All circles (black and open) and 'X's denote electrode penetration locations. Black circles represent sites where neurons responded to the stimulation of deep receptors on the contralateral body surface. Open circles represent sites where neurons responded to the stimulation of cutaneous receptors. 'X's mark locations of no clear neuronal response. Squares denote lesions made during the recording experiments. Thick lines represent cortical boundaries determined from myeloarchitectonic analysis, or myeloarchitectonic and electrophysiological analysis combined. Thin lines mark boundaries between body part representations. See Table 1 for abbreviations. Medial is up, and rostral is to the left, scale = 1 mm.

Table 1
List of abbreviations

Cortical areas and regions

A1	primary auditory area
Cing	cingulate cortex
DM	dorsal medial area
FST	fundal superior temporal area
M1	primary motor area
MST	medial superior temporal area
MT	middle temporal area
PM	premotor area
PP	posterior parietal cortex
PV	parietal ventral area
R	rostral auditory area
S1	primary somatosensory area
S2	second somatosensory area
SMA	supplementary motor area
V1	primary visual area
V2	second visual area
VPP	ventral posterior parietal area

Body parts

ank	ankle
ch	chin
d	digit
fa	forearm
fl	forelimb
ft	foot
el	elbow
ha	hand
hl	hindlimb
glab	glabrous
ll	lower lip
nb	nail bed
nk	neck
sh	shoulder
t	toes
ton	tongue
tr	trunk
ul	upper lip
wr	wrist
vb	vibrissae

Direction terms

di	distal
dor	dorsal
pr	proximal
lat	lateral
low	lower
up	upper
M	medial
R	rostral
ven	ventral

recording results and areal patterns of connections. All experimental protocols were approved by the Animal Use and Care Administrative Advisory Committee of the University of California, Davis, and conformed to NIH guidelines.

Surgery and Injections

In all cases in which anatomical connections were studied, sterile surgical procedures were followed. Prior to surgery, each animal was anesthetized with ketamine hydrochloride (30 mg/kg, i.m.) and xylazine (2 mg/kg, i.m.). Dexamethasone (0.2 mg/kg, i.m.), and atropine (0.1 mg/kg, i.m.) were also administered to prevent edema and increase heart rate, respectively. Additional doses of ketamine hydrochloride (half of initial dose) were administered as needed to maintain a surgical level of anesthesia. Lidocaine (0.05–0.1 ml of 2%) was injected subcutaneously near the ear canals where the ear bars were inserted. During surgery, heart rate, respiration rate and body temperature were monitored.

Once anesthetized, the skin was cut, the temporal muscle retracted, and a craniotomy was performed over somatosensory cortex. For the

cases in which extensive electrophysiological recordings were made, an acrylic well was placed around the opening and filled with silicone fluid to help maintain cortical temperature and prevent desiccation. A photograph of the exposed cortical surface was taken to relate electrode penetration sites, lesions, and probes to blood vessel patterns. Multi-unit recording techniques were used to determine the location of area 3a, and the receptive fields (RFs) for neurons where injections were centered. Calibrated Hamilton syringes were used to inject 0.3–0.5 µl of 7% fluororuby (FR; Molecular Probes, Eugene, OR), 0.3–0.5 µl of 7% fluoroemerald (FE; Molecular Probes) or 0.05 µl of a 0.1% wheat-germ agglutinin conjugated to horseradish peroxidase solution (WGA-HRP; Sigma, St Louis, MO). All tracers were diluted in water. After completion of the injections, a sterile contact lens was placed over the exposed cortex, the cut dural flaps were placed over the lens, and the skull opening was covered by a skull cap made of dental acrylic. The cranial muscles were sutured, the skin was sutured, and each animal was monitored closely during the 6–7 day recovery period for transport of tracers.

Electrophysiological Recordings

Multi-unit neuronal recordings were obtained at depths of 500–700 µm from the pial surface, approximately in layer IV, with low-impedance tungsten-in-glass microelectrodes (0.95–1.5 MΩ at 100 Hz). The electrode entered the cortex perpendicular to the cortical surface and a stepping microdrive was used to advance the electrode. Once the electrode was in place, the entire body surface was stimulated and the RF for neurons at that site was determined and drawn on a picture of the body. Stimulation consisted of displacement of hairs, light brushing of skin surfaces, joint and limb manipulation, pressure, and light to moderate taps. In three cases (96-12, 96-8, 00-16), a complete representation of the contralateral body surface was identified; in four additional cases (00-17, 00-18, 00-19, 96-9; not shown), partial topographic maps were defined. Electrolytic lesions (10 µA for 10 s) were made at the judged physiological boundaries of area 3a for later identification in histologically processed tissue. Additionally, small probes (pasta) were inserted into the cortex at the boundaries of somatosensory cortex and marked on the photograph of the exposed neocortex to further aid in reconstructing electrophysiological data and anatomical results.

Histological Processing

Following a 1-week recovery period, marmosets in which an anatomical tracer was injected were administered a lethal dose of sodium pentobarbital (IP). It was perfused transcardially with 0.9% saline in 0.1 M phosphate buffer, followed by 2% paraformaldehyde in phosphate buffer (pH 7.4), and then 2% paraformaldehyde in 10% sucrose phosphate buffer. This procedure was also implemented immediately following the electrophysiological recording in the acute cases, and the two cases where maps were obtained in addition to the injections of tracers. After the brain was removed from the skull, the corpus callosum was transected, each cortical hemisphere was peeled from the brainstem and thalamus, the lateral sulcus was opened, the medial wall was retracted, and the cortex was manually flattened with a glass slide in a large Petri dish filled with 2% paraformaldehyde in 30% sucrose phosphate buffer. All cortices except case 00-16 (WGA-HRP) were post-fixed for 2 days, then each flattened cortex was frozen onto a microtome stage, and cut parallel to the cortical surface into 40 µm sections. Alternate sections were mounted for fluorescent analysis, and stained for myelin (Gallyas, 1979). For case 00-16 where WGA-HRP was injected into area 3a, a series of sections was reacted for tetramethylbenzidine (TMB) (Mesulam, 1978).

Data Analysis

To determine the somatotopy of area 3a, neuronal RFs and the type of stimulus that best drove the neurons at all recording sites were related to the photographs of the brain in which sites were plotted. Although some characteristics of the neural response such as rapidly adapting or slowly adapting properties were observed and documented, no clear pattern in their distribution emerged and were excluded from the maps. Receptive field progressions, reversals and changes in the optimal stimulus defined physiological boundaries of area 3a. The recording sites, corresponding RFs, and optimal stimulus for each recording site were transposed onto a single somatotopic map of area 3a for each case. Reconstructions of

the sections stained for myelin were related to the physiological maps by matching blood vessel patterns, lesions and probes. In all cases, we determined cortical area boundaries by combining electrophysiological recordings results with myeloarchitectonic distinctions. The entire series of sections stained for myelin was used to determine cortical field boundaries. Using a camera lucida attached to a light microscope, the boundaries of cortical areas were drawn based on subtle to extreme variations in myelination. Many of these areas that are defined using the technique described above have been previously correlated with electrophysiologically identified areas (Aitkin *et al.*, 1986; Carlson *et al.*, 1986; Krubitzer and Kaas, 1990a; Fritsches and Rosa, 1996; Rosa *et al.*, 1997; Luethke *et al.*, 1989). To determine cortical fields boundaries with accuracy, multiple criteria should be used (Kaas, 1982). In our study, we used a combination of electrophysiological recording techniques, cortical myeloarchitecture, and neuroanatomical tracing of connections.

For the analysis of the brains injected with fluorescent tracers, a fluorescent microscope, attached to a personal computer equipped with MDPLOT optical plotting system software (Minnesota Datametrics Corporation, St Paul, MN) was used to plot injection sites and retrogradely labeled cell bodies in the cortex (Fig. 11*d-f*). For the analysis of the brain injected with WGA-HRP, a light microscope equipped with polarizing filters and a camera lucida was used to plot the locations of labeled cell bodies and axon terminals. The outline of each section, the blood vessels, lesions, probes and labeled cells were individually drawn and related to one another. These reconstructions were co-registered with the cortical myeloarchitecture (from the myelin sections) using blood vessel patterns and artifacts produced from lesions and probes as guides. All sections were drawn at the same magnification in order to facilitate the correlation of the anatomical and physiological data.

Results

Internal Organization of Area 3a

In the present investigation, densely spaced recording sites in the anterior parietal cortex of marmoset monkeys allowed us to delineate a region where neurons responded to the stimulation of deep receptors. This region, area 3a, was ~12–14 mm in its medio-lateral extent, 1–2.5 mm in its rostrocaudal extent, and contained a complete representation of the sensory receptors (Figs 1 and 2). The mediolateral organization of area 3a was similar to area 3b with the tail represented most medially, followed by the foot and hindlimb representations. The trunk, forelimb, hand and digit representations were found more laterally, followed by the representations of the chin, face and oral structures.

Although we did not quantify our data, there were several features of the neural response that could be readily documented. First, under our anesthetic conditions, neurons in area 3a responded well to stimulation of deep receptors and were non-habituating. While we observed both rapidly adapting (RA) and slowly adapting (SA) responses of neurons in area 3a, often for neurons at the same recording site, it was not possible to tease out individual neuronal adapting properties. Further, unlike area 3b, there was no clear pattern of RA and SA bands in area 3a. Similarly, neurons responded well to very light taps of different body parts as well as muscle stretch, but it was difficult to separate the two under our recording conditions, and there appeared to be no clear pattern of response preference of neurons across area 3a. To address these issues, single unit recordings in area 3a are required.

Three detailed maps (Figs 1*b,c* and 3) and four partial maps (Fig. 6*a*; others not shown) were obtained. In all cases, the electrophysiological results were combined with myeloarchitectonic boundaries (see below). Within the tail representation, the distal tail was located medial to the proximal tail. In cases 96-12 and 96-8, the foot representation abutted the

representation of the tail, although in one case, a small hindlimb representation also adjoined the tail representation (Fig. 1). The representation of the toes was in one case lateral (Fig. 1*b*), in one case caudal (Fig. 1*c*), and in two cases medial (Fig. 2; other case not shown) to the representation of the foot. In an additional case, the representation of the toes was both medial and lateral to the representations of the foot (not shown). In all cases the glabrous distal toes were represented at the caudal boundary of area 3a, and adjoined the distal toe representation in area 3b (Figs 1 and 2). Neurons in the rostral portion of the toe representation of area 3a had RFs on the dorsal surface, while neurons in the caudal portion of the toe representation had RFs on the glabrous surface. Just lateral to the representations of the foot and toes was the representation of the hindlimb, and lateral to this was the trunk representation.

The forelimb representation in area 3a, which included the representations of the proximal forelimb, elbow, shoulder, wrist and hand occupied approximately one-third of the entire field. Within the forelimb representation, the proximal forelimb was represented just lateral to the trunk and hindlimb in two cases (Figs 1*b* and 2). In another case, the forelimb, elbow and wrist were represented rostral and caudal to the trunk representation and lateral to the hindlimb representation (Fig. 1*c*). The hand representation, which included the digits, dorsal hand and the glabrous palm, was located lateral to the forelimb, and the digit representation was located lateral to the hand and forelimb representations in all cases (Figs 1 and 2). Within the representation of the digits, the ulnar digits were located medial to the radial digits. As in the representation of the toes, the distal digits were represented at the caudal boundary of area 3a and adjoined the representation of the distal digit tips in area 3b. In one case (Fig. 1*b*), the shoulder was represented rostro-lateral to the digits.

Lateral to the representation of the digits was the representation of the face and oral structures. Within the representation of the face, the chin was located most medially, and adjoined the representation of the digits of the hand. Lateral to the chin were the representations of the lips and teeth, and in one case (00-16) the tongue (Figs 1 and 2). In case 96-12, the snout was represented rostral to the representation of the chin (Fig. 1*b*).

Although the internal organization of area 3a consistently mirrored that of 3b, the details of the internal organization described above were variable among animals. For example, in two cases the forelimb representation was large and contiguous (Figs 2*a* and 3); in another case, it was broken into two islands, one rostral and one caudal to the trunk representation (Fig. 1*c*). Likewise the representations of the digits were variable in all cases, although the relative location with respect to the rest of the body part representations was consistent across cases (e.g. compare the digit representations in Figs 1*b*, 1*c* and 2). Because our sampling density was high, we believe that the variation observed for the two fields was not a result of experimental error or paucity of data, but reflected true variability in the maps of area 3a in the two animals described.

Electrophysiological recordings were also made rostral and caudal to area 3a. In cortex rostral to area 3a, in M1, most neurons were unresponsive to any type of somatic stimulation. However, in two cases (Figs 1*b* and 2), neurons responded to stimulation of deep receptors at a few recording sites. The lack of response of neurons to somatic stimulation in M1 is counter to previous reports in awake monkeys in which neurons in M1 did respond to somatic stimulation (Tanji and Wise, 1981; Wise and Tanji, 1981). However, this difference is likely due to our anesthetized preparation.

00-16 LH

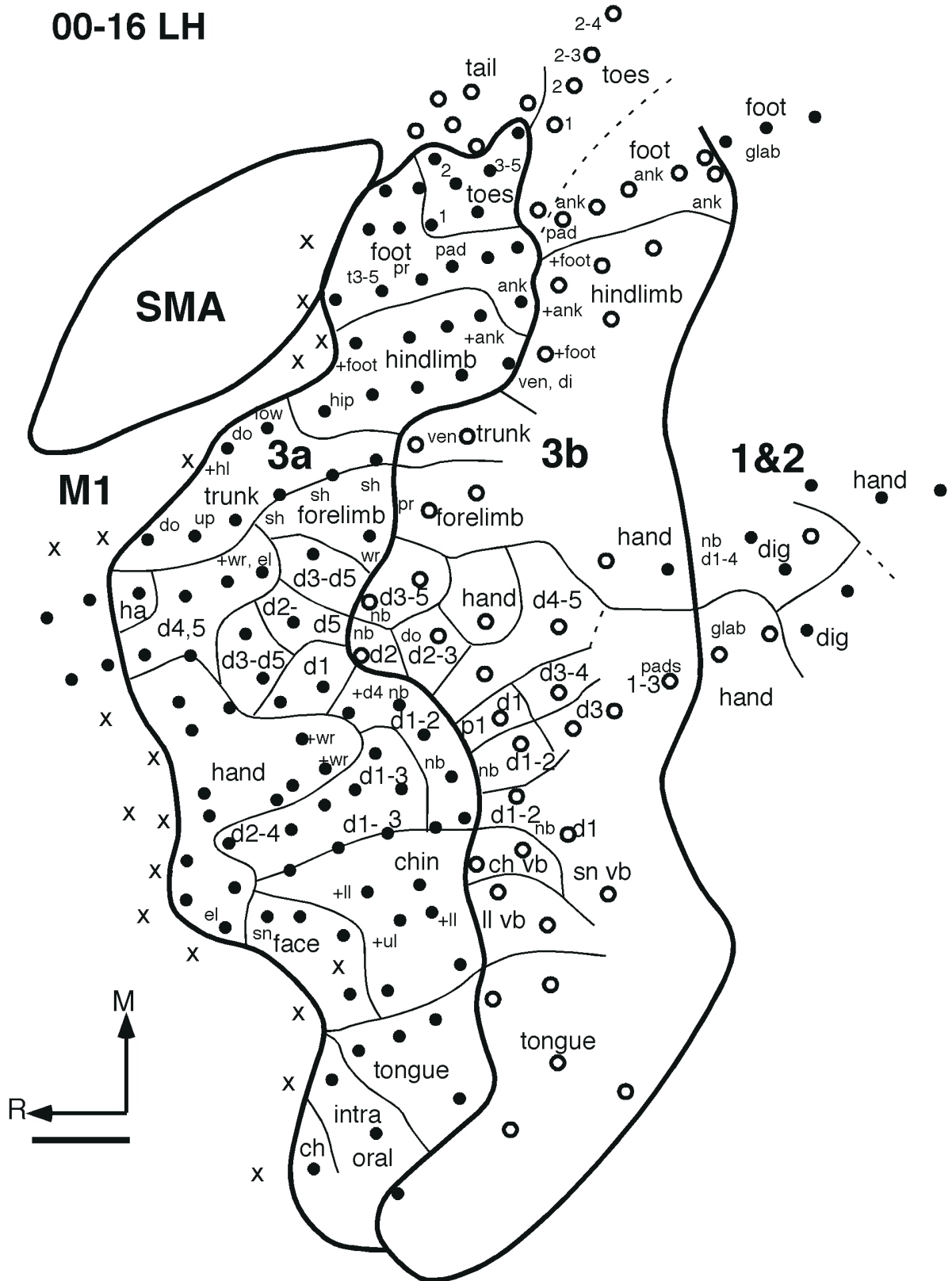


Figure 2. A map of area 3a, and neighboring cortex in the flattened left hemisphere of case 00-16. Although the general topographic organization of area 3a in this case is similar to that shown in other cases (Fig. 1), the physiological boundaries between body part representations are in different relative locations. All conventions are as in the previous figure.

Caudal to area 3a, neurons responded well to stimulation of cutaneous receptors (Figs 1 and 2). Neurons at these recording sites tended to have smaller RFs than neurons in area 3a,

although this was not systematically studied. When matched to cortical myeloarchitecture, these neurons were found to be in area 3b. Finally, neurons caudal to area 3b were recorded in areas

1 and 2. Some neurons in this region responded to cutaneous stimulation, but most responded to stimulation of deep receptors (e.g. Fig. 2; other cases not shown).

Receptive Fields for Neurons in Anterior Parietal Cortex

The physiological borders of area 3a were characterized by a lack of neural responsiveness, or changes in the class of receptors stimulated which produced a neural response, and reversals in the location of RF progression. For example, for the forelimb representation in case 96-12 LH (Fig. 3), the locations of RFs for neurons changed from the elbow, onto the glabrous hand, digits and then digit tips in a rostral to caudal progression of recording sites in area 3a (Fig. 3, RF 1-4). At the 3a/3b border, locations of RFs for neurons progressed from the distal digit tips, back onto all of the digits, then onto the glabrous palm, and finally onto the forearm in a rostral to caudal progression of recording sites in area 3b (Fig. 3, RF 5-8).

Similar types of reversals and changes in the type of receptor

represented were observed for the map of the face. As recording sites moved from rostral to caudal in area 3a, the location of RFs for neurons at those sites moved from the lateral face and cheek onto the lips and chin (Fig. 4, RF 1-3). At the 3a/3b border, the location of RFs for neurons were on the chin, and then moved back onto the side of the face (Fig. 4, RF 4-6). Although clear reversals were not observed for the representation of the toes, the location of RFs for neurons in area 3a progressed from the foot, onto the distal glabrous toes from rostral to caudal. At the 3a/3b boundary, the location of RFs for neurons remained on the distal glabrous toes, and then moved back onto the hairy foot as recording sites progressed from rostral to caudal (Fig. 3, RF a-h).

For all examples described above, as recording sites crossed the 3a/3b border, a change in the optimal stimulus was observed. Area 3a neurons responded to stimuli that activated deep receptors such as muscle spindles and deep skin receptors, and 3b neurons responded to stimuli that activated cutaneous skin receptors. Also, as recording sites progressed across the

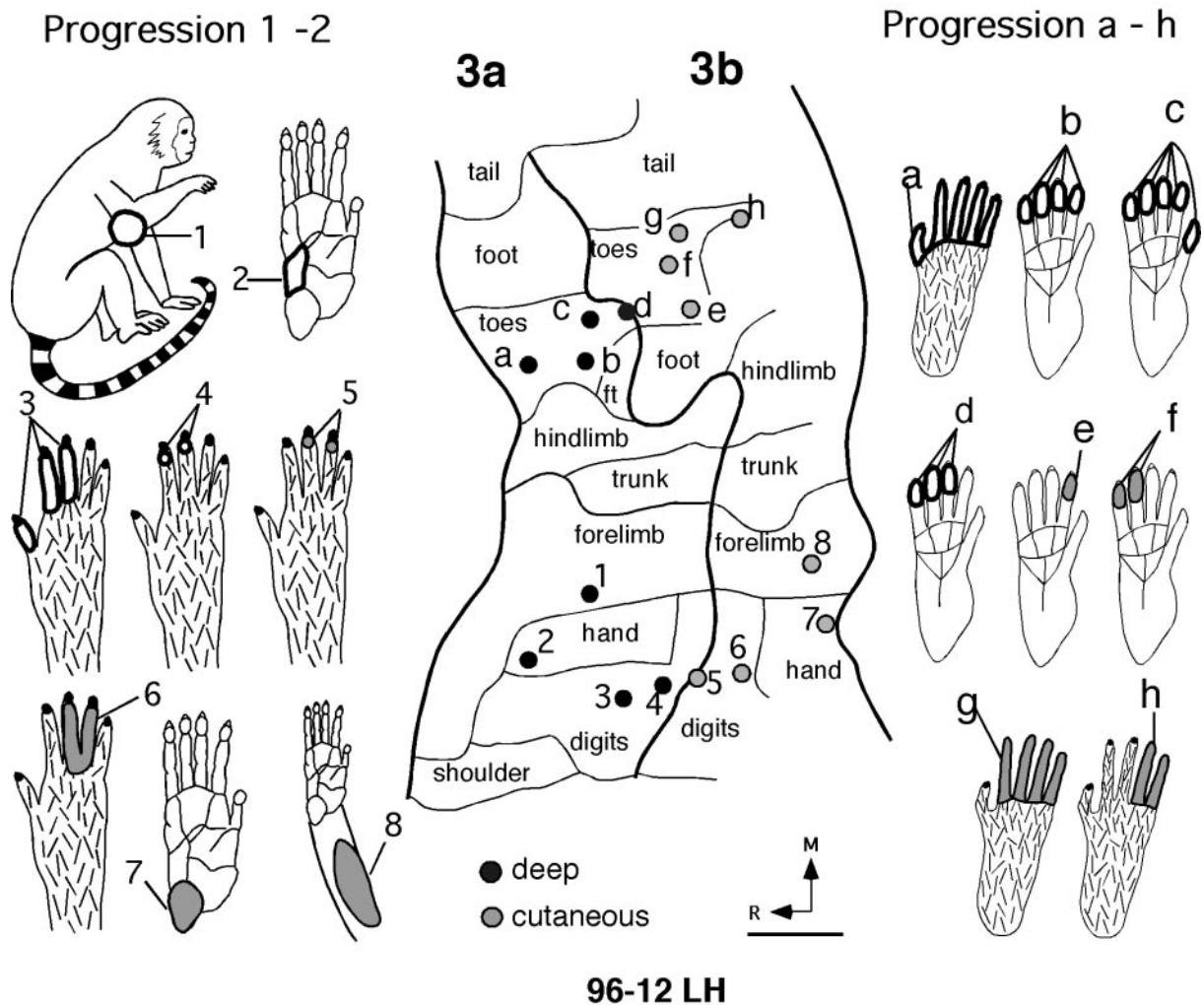


Figure 3. Receptive field progression and reversal in the forelimb representation in the left hemisphere of case 96-12. Recording sites in 3a and 3b are numbered from 1 to 8 on the cortical map (middle). The corresponding RFs for neurons at those sites are drawn on the contralateral body surface (left). Black circles denote locations where neurons responded to the stimulation of deep receptors, and gray circles denote locations where neurons responded to the stimulation of cutaneous receptors. As recording sites move from area 3a into 3b, locations of RFs progress from the elbow, to the glabrous palm, to the digits, to the distal digits (sites 1-4). At the 3a/3b border, the locations of RFs reverse and progress from the distal digits, to the digits, onto the glabrous palm, and then onto the ventral forelimb (5-8). Receptive field progression and reversal in the representation of the toes are shown for recording sites a-h (middle), and corresponding RFs for neurons at those sites are shown on the right. As recording sites move from area 3a into 3b, RFs progress from the foot, to the glabrous distal toes (a-d). As recording sites cross the 3a/3b border, the RFs progress from the distal glabrous toes, back onto the dorsal toes (e-h). Conventions as in previous figures.

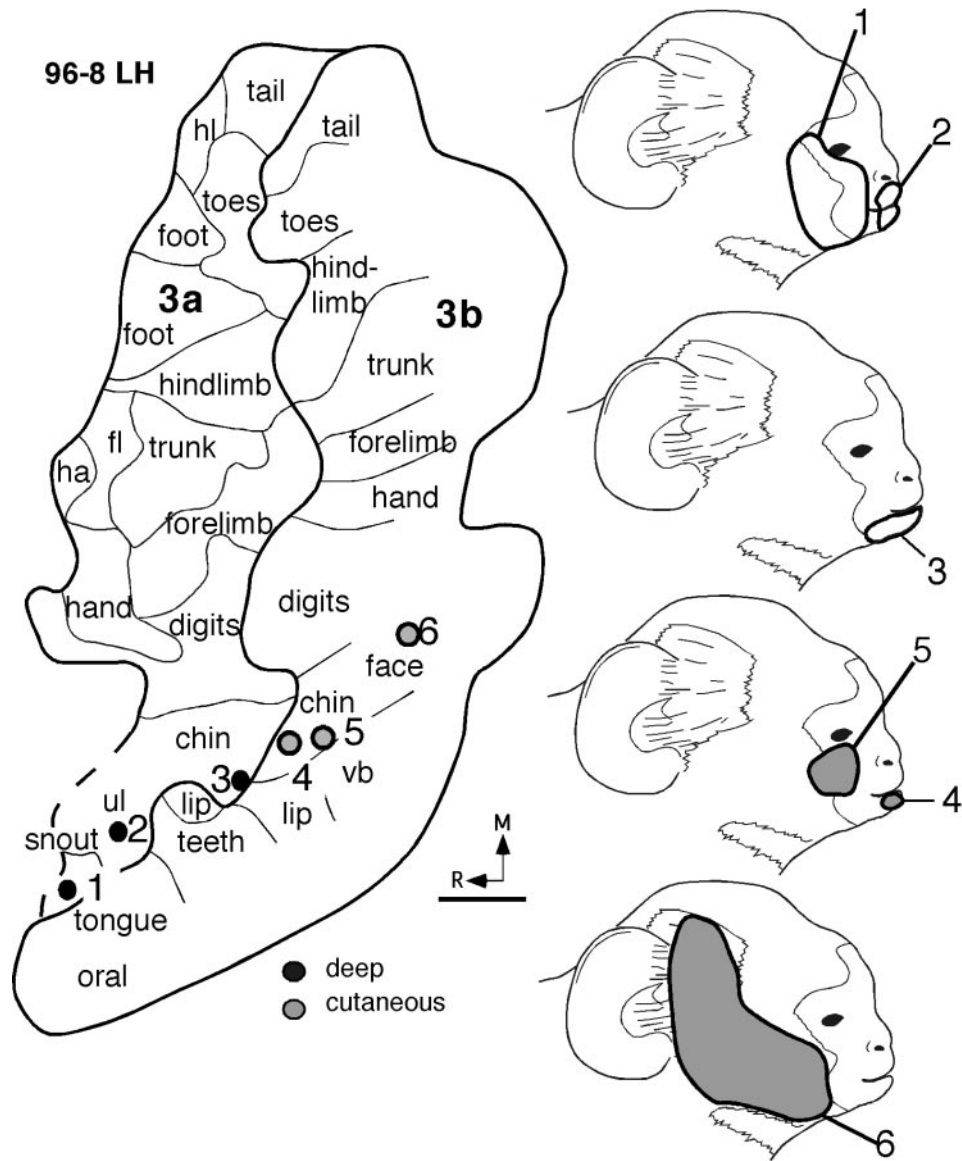


Figure 4. Receptive field progression and reversal in the face representation in the left hemisphere of case 96-8. Recording sites in areas 3a and 3b are shown on the left, and the corresponding RFs on the face for neurons at these sites are on the right. As recording sites move from area 3a into 3b, locations of RFs progress from the lateral face, or cheek, to the lips and chin (1–43). As recording sites cross the 3a/3b border, locations of RFs reverse and move from the chin, onto the cheek, or lateral face, and onto the lateral face (4–6). Conventions as in previous figures.

border, the location of RFs for neurons at those sites reversed, and a re-representation of RFs for the different classes of receptors (deep and cutaneous) was observed at different locations in the cortex. This re-representation could be readily observed when similar RF locations were directly compared for areas 3a and 3b (Fig. 5). For instance, similar RF locations on the hindlimb could be observed for neurons at recording sites separated by over 2.5 mm (Fig. 5, compare RFs 1 and A). This was true for all body parts. There was a tendency for the RF of neurons to be larger in area 3a than in 3b (e.g. Fig. 3, compare RFs b and c with RFs e and f; Fig. 5 compare RF D with RF 4), but this was not systematically studied.

Intrinsic Connections of Area 3a and Ipsilateral Connections with Somatosensory Cortical Areas

The connections of area 3a were determined by injecting

fluorescent tracers or WGA-HRP into electrophysiologically defined locations (Figs 6–9, 11e,f). In one case (96-9 LH), more extensive electrophysiological recordings were made so that the projections from different body part representations to a given site in area 3a could be determined (Fig. 6a). In this case, fluoroemerald was injected into the hindlimb representation (specifically, a cluster of neurons with a RF on the dorsal distal hindlimb), with some spread into the trunk and shoulder representations (Fig. 6a, medial injection site). Fluororuby was injected into the forearm representation, and the injection spread into the wrist and hand representations (Fig. 6a, lateral injection site, see Fig. 17f for digital image of FR injection site). The hindlimb/trunk representation in 3a received dense input from portions of the hindlimb, trunk and shoulder representations in 3a (Fig. 6b, also see Fig. 8). Connections between similar body part representations such as the hand and hand or hand and

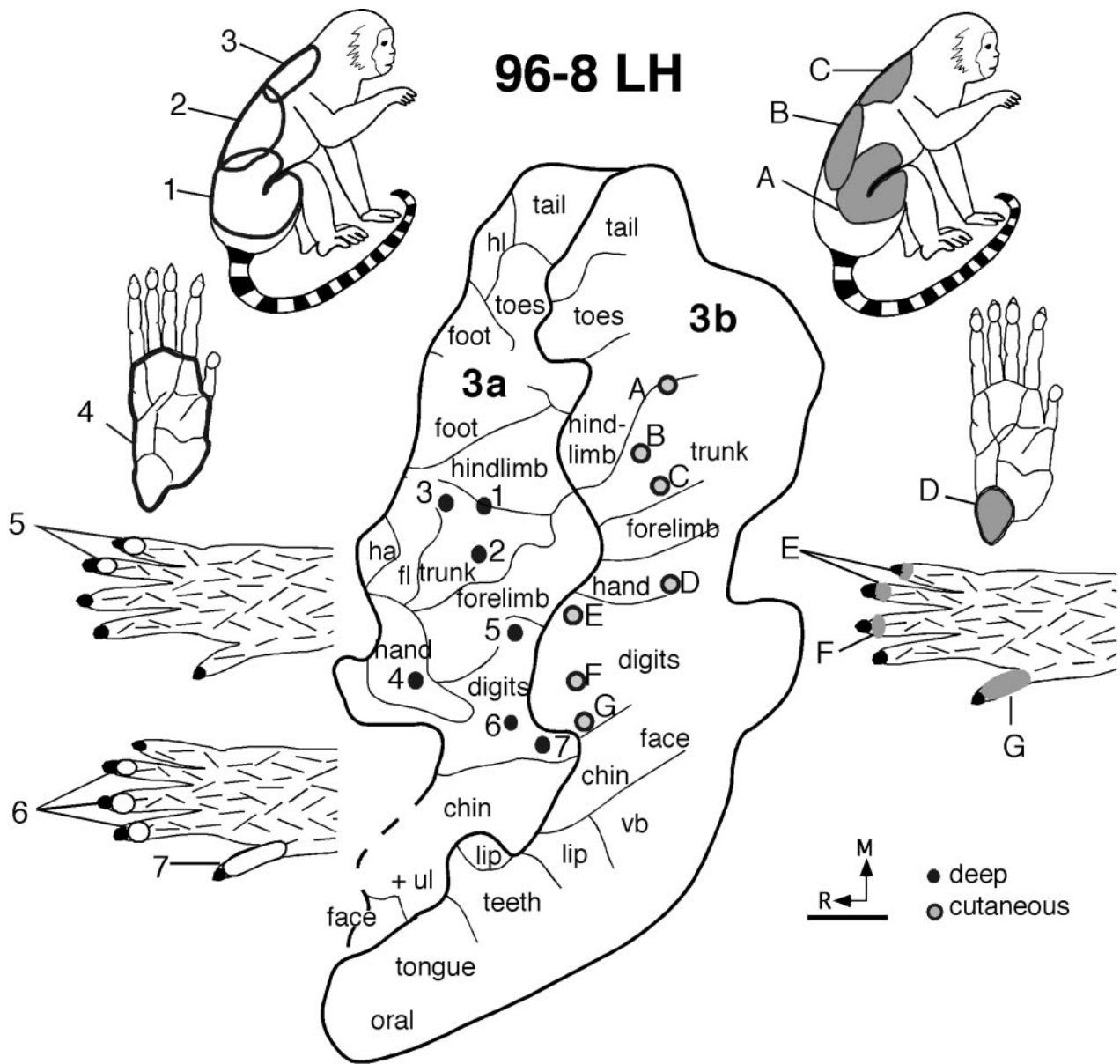


Figure 5. Receptive field re-representation in areas 3a and 3b in the left hemisphere of case 96-8. Recording sites in areas 3a and 3b (middle) are shown with the corresponding RFs for neurons at those sites on the contralateral body in area 3a (left) and 3b (right). Clusters of neurons at distantly located recording sites have similar RFs, but respond to the stimulation of different types of receptors (cutaneous vs deep). For example, recording sites 2 and B are over 2 mm apart, and neurons at these sites have RFs on a similar location on the trunk. Comparison of RFs for neurons at the other recording sites demonstrates a similar re-representation. Conventions as in previous figures.

forelimb we term 'matched'. The hindlimb/trunk representations in area 3a also received moderate input from the hand, and digit representations, and very sparse input from the face representation in 3a (Fig. 6b). Connections such as this, between very different body part representations (e.g. hand and hindlimb) we term 'mismatched'. A number of retrogradely labeled cells were also observed in a caudal location, in areas 1 and 2. These cells were in the expected location of the hindlimb and trunk representations, and thus were matched. A few labeled cells were observed in a lateral location in area 1 and 2, in the expected location of the face and digit representations. Area 3b contained labeled neurons at its rostral and caudal border in matched representations. Finally, a few labeled cells were

observed in the parietal ventral area (PV) and S2. In case 96-11, in which an injection of fluoroemerald was placed in the representation of the trunk/hindlimb in area 3a, similar patterns of intrinsic and extrinsic connections to those described above were observed (see Fig. 11e for a digital image of this FE injection site). Label in areas 3b, 1 and 2 was mostly matched (Fig. 8). In this case, there was very dense labeling in S2, and only sparse labeling in PV.

Results were similar for the injection of fluororuby in case 96-9 (Fig. 6c, see Fig. 11d for a digital image of a FR-labeled cell). The forearm, wrist and hand representations in 3a received matched input from these same representations in 3a, as well as dense input from the digits and shoulder representations, and

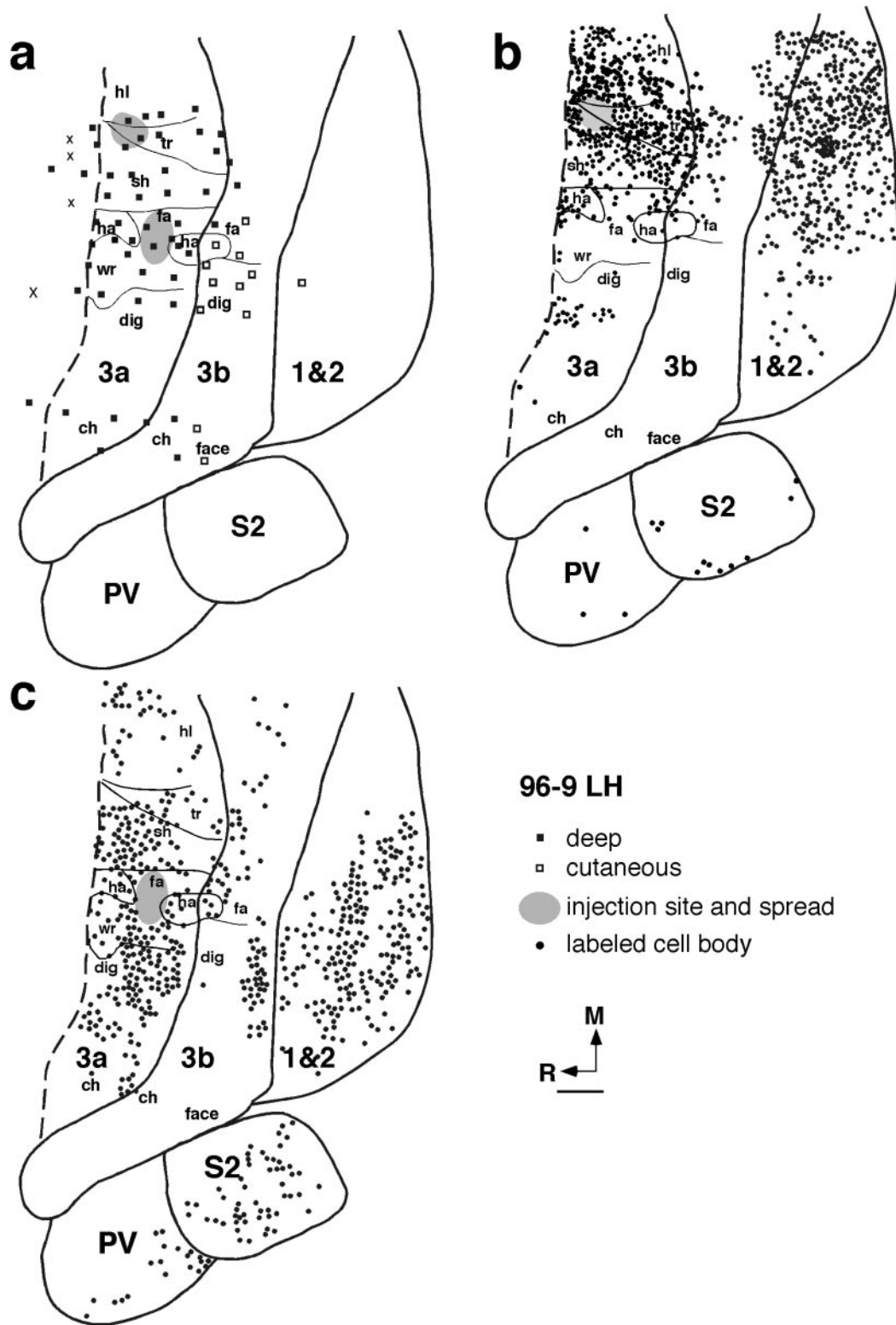
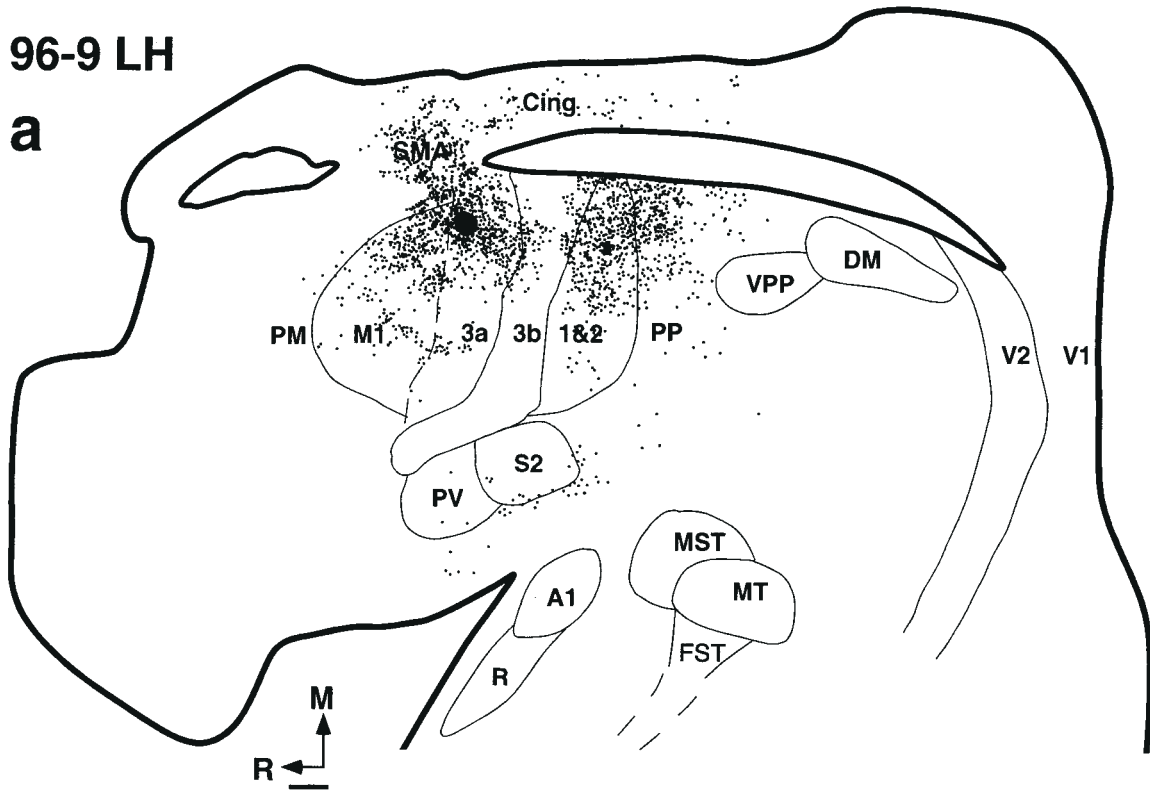


Figure 6. A partial map of area 3a that depicts the center of two injection sites and their spread (*a*) in relation to body part representations, and the intrinsic connections resulting from those two injections (*b* and *c*) in case 96-9. In (*a*) an injection of fluoroemerald (FE) was centered in the representation of the hindlimb but spread into the trunk and slightly into the shoulder representations (medial injection site). An injection of fluororuby (FR) was centered in the representation of the forearm but spread into the hand and wrist representations (lateral injection site). In (*b*), the most dense connections of the trunk/hindlimb representation in area 3a are with closely related representations (such as the rest of the hindlimb and trunk), and with mismatched representations in area 3a (such as the hand, forearm and face). Label is also observed in the expected location of the trunk, hindlimb and forelimb representation in areas 1 and 2. In (*c*), a similar pattern of matched and mismatched connections was observed for the representation of the forearm in area 3a. However, the extent of mismatched label appeared to be greater for the injection in the representation of the forearm when compared with the injection in the representation of the hindlimb. Solid circles represent retrogradely labeled cell bodies from each of the two injections (*b* and *c*). Solid squares represent electrode penetration locations where neurons responded to the stimulation of deep receptors, and open squares represent locations where neurons responded to the stimulation of cutaneous receptors (*a*). Thick lines mark architectonic boundaries, or boundaries determined using both architectonic analysis and electrophysiological analysis. Other conventions as in previous figures.

96-9 LH

a



b

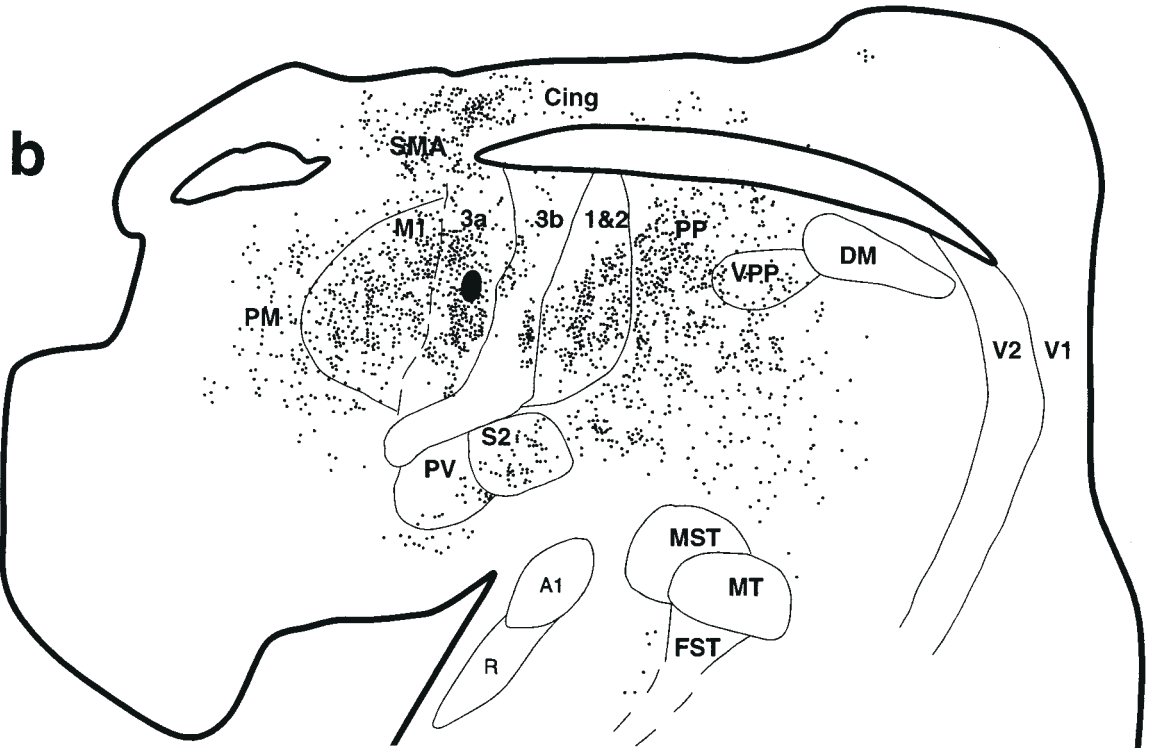


Figure 7. Complete reconstructions of the two injections described in Figure 8 in case 96-9. In (a), an injection of FE centered in the representation of the hindlimb resulted in densely labeled cell bodies in areas 1 and 2, PP, SMA and M1. Sparse to moderate label was observed in 3b, PM, cingulate cortex, M, PV and S2. In (b), an injection of FR that was centered in the forearm representation resulted in dense labeling in areas 1 and 2, M1, PP and SMA. Moderate to sparse label was observed in 3b, M, VPP, cingulate cortex, PM, SI and PV. In this case, a few labeled cell bodies were observed just rostral to FST. Conventions are as in previous figures.

moderate inputs from the hindlimb, trunk and face representations in 3a. Input from areas 3b, 1 and 2 was diffuse and spread across most body part representations in these fields. Input from

both S2 and PV was much more dense than for the hindlimb representation injections (Fig. 6c).

In case 00-16, in which WGA-HRP was injected into area 3a,

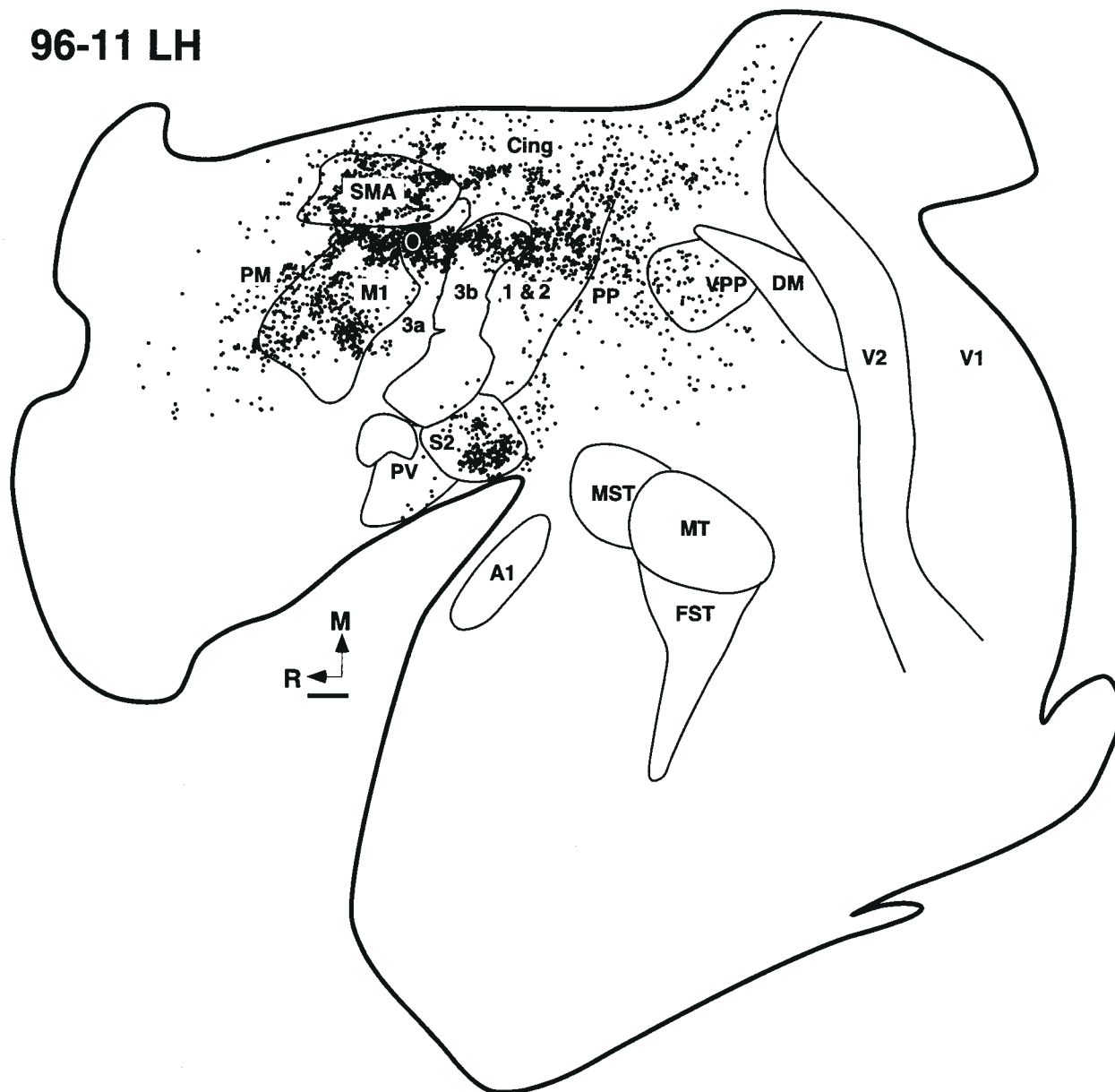


Figure 8. A reconstruction of an injection in case 96-11. An injection of FE was placed in the representations of the trunk/hindlimb of area 3a. The patterns of label were similar to those described for the case illustrated in Figure 9. Conventions as in previous figures.

patterns of both anterograde and retrograde connections were determined. The hand representation in area 3a projected to matched and mismatched regions of area 3a (compare Fig. 9 with Figs 6c and 7b). There were sparse projections to the matched representation in area 3b, and to the presumptive face representation in 3b. Areas 1 and 2 received matched input from the hand representation in area 3a.

Ipsilateral Connections with Motor, Posterior Parietal and Cingulate Cortex

Area 3a did not only receive input from somatosensory areas, it also received substantial input from cortical regions associated with processing motor outputs such as the primary motor cortex (M1), the supplementary motor area (SMA), and the premotor cortex (PM) (Figs 7-9). While M1 and SMA were myeloarchitecturally distinct (see below), in our preparation the cortex

rostral to M1 was not. However, cortex immediately rostral to M1 has been described as PM in other New World monkeys (Stepniewska *et al.*, 1993; Preuss *et al.*, 1996). Therefore, this region was termed PM, although it is likely that it contains additional subdivisions, such as the frontal eye fields. Injections into medial portions of area 3a in the representation of the hindlimb and trunk resulted in dense label in more medial portions of M1, and sparse label in lateral portions of M1 (Figs 7a and 8). Injections into the forelimb representation in area 3a resulted in broadly distributed label in M1 and SMA (Figs 7b and 9). Label in PM that resulted from injections into different body part representations into area 3a was sparsely distributed throughout the field (Figs 7 and 8).

Posterior parietal cortex (PP) also provided dense input to area 3a. Labeled cells in PP were found throughout its extent, but were concentrated at a mediolateral location similar to that

b. 00-16 RH

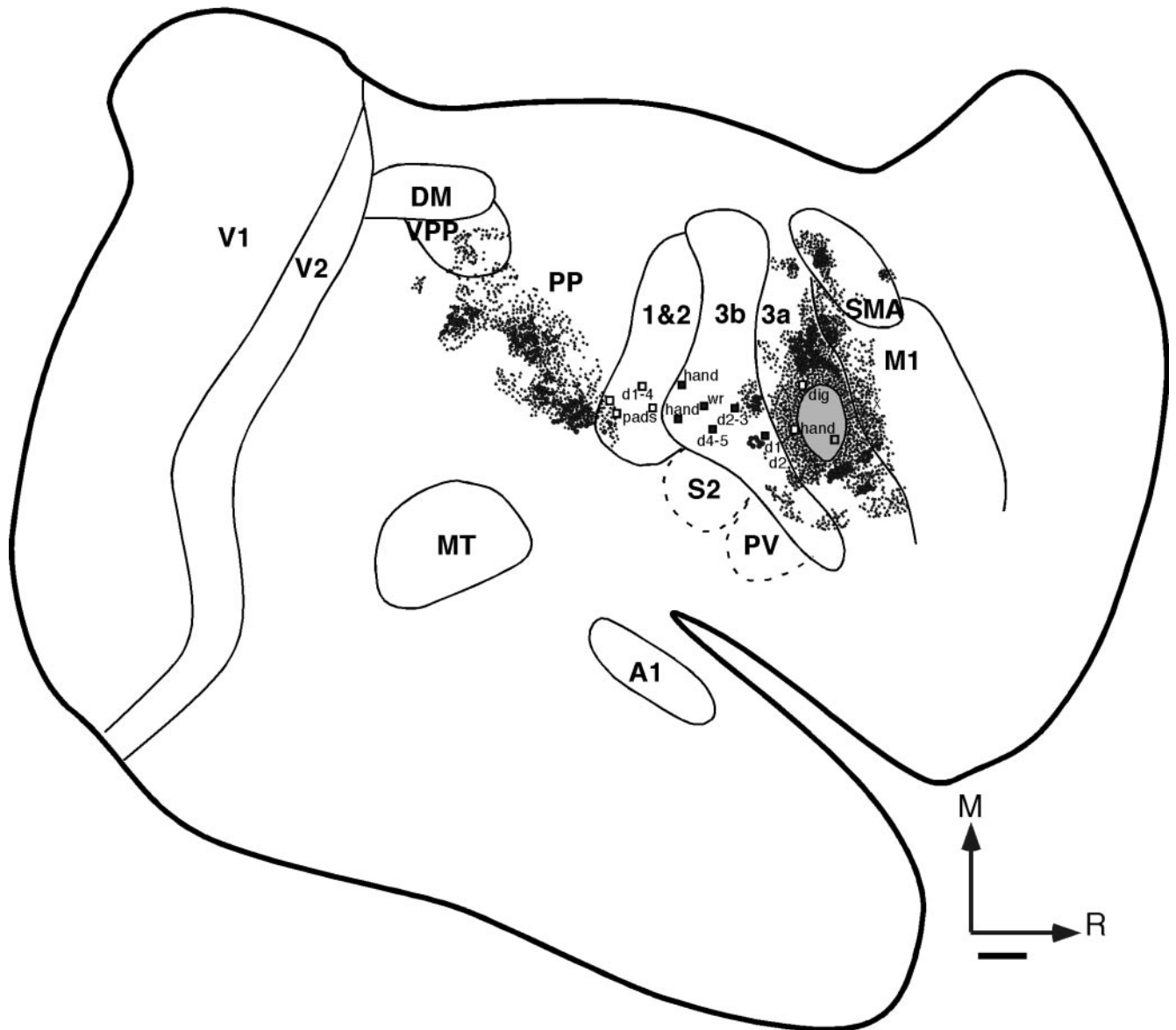


Figure 9. A reconstruction of an injection of WGA-HRP and labeled cells and terminals in case 00-16. The injection was centered in the representation of the hand in area 3a. The hand representation of area 3a was interconnected with matched and mismatched representations in area 3a, M1 and PP, and to predominantly matched locations in areas 3b, 1 and 2. Small dots represent axon terminals (anterograde label) and large dots represent cell bodies (retrograde label). The open squares denote electrode recording locations where neurons responded to the stimulation of deep receptors. The solid squares denote locations where neurons responded to the stimulation of cutaneous receptors. All conventions as in previous figures.

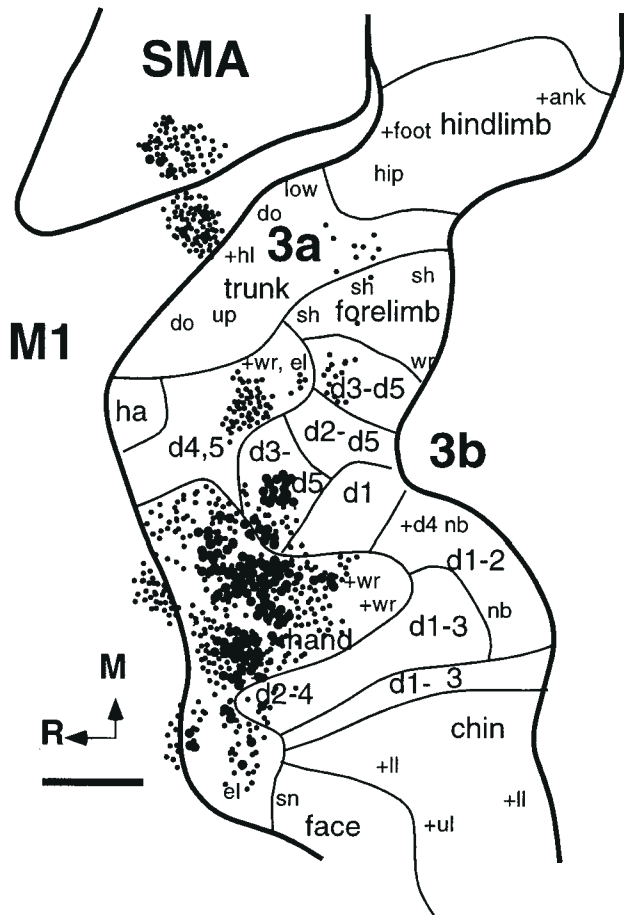
injected in area 3a; this suggested that PP may have some type of topographic organization. Thus, injections into the medial portion (in the hindlimb/trunk representation) of area 3a resulted in densely labeled cell bodies in a medial location in posterior parietal cortex, although there was sparse label in lateral portions of PP (Figs 7a and 8). Injections into the laterally located forelimb representation resulted in dense label throughout the extent of PP (Figs 7b and 9). An area generally associated with visual processing (Krubitzer and Kaas, 1993; Beck and Kaas, 1998) was located caudal to PP and termed the ventral posterior parietal area (VPP). For three injections, sparse label was observed in VPP (Figs 7b, 8 and 9). Finally, in most cases, the cingulate cortex, which was located on the medial wall just

dorsal to the corpus callosum, contained a light scattering of labeled cell bodies (Figs 7a,b and 8).

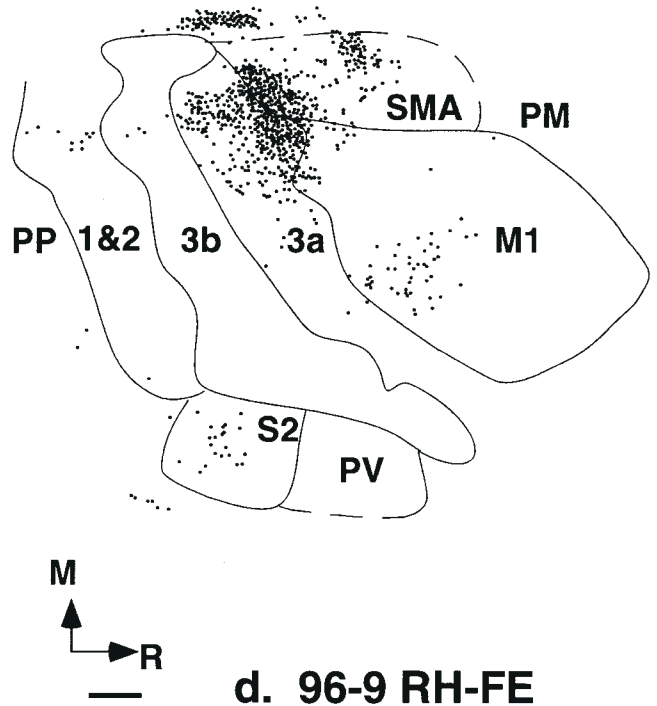
Contralateral Input to Area 3a

In all cases, the majority of contralateral input to area 3a was from a location that corresponded to that injected in the other hemisphere. In case 00-16, we mapped the extent of area 3a in the hemisphere opposite to the injection in the hand representation in area 3a (Fig. 10a). The hand representation in area 3a was interconnected predominantly with 3a hand representation in the contralateral hemisphere, the various digit representations and the trunk representation. Finally, area 3a was interconnected with M1 and SMA contralaterally. In the

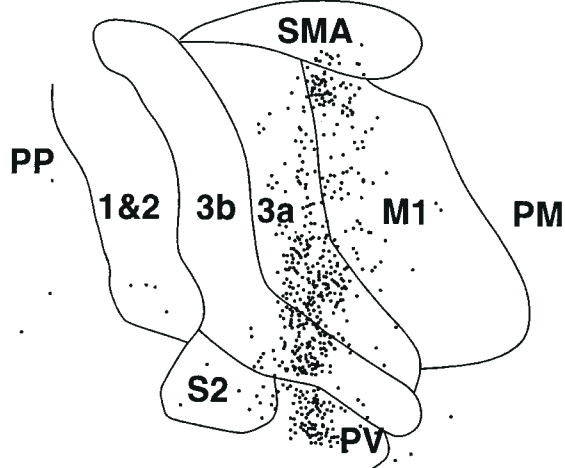
a. 00-16 LH



b. 96-11 RH



c. 96-9 RH- FR



d. 96-9 RH-FE

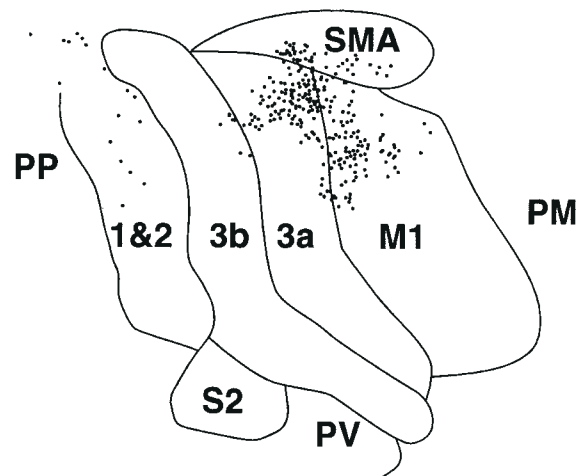


Figure 10. Reconstruction of retrogradely labeled cells (large dots) and axon terminals (small dots) relative to electrophysiologically defined body part representations (thin lines) and myeloarchitectonic boundaries (thick lines) in the contralateral flattened left hemisphere of case 00-16 (a). The injection in this case was placed in the hand representation, which is densely interconnected with the hand representation in 3a of the opposite hemisphere (shown here). Also, clusters of terminals were observed in different digit representations, the forelimb representation and the trunk representation in 3a. The hand representation in area 3a is also interconnected with SMA and M1 of the opposite hemisphere. The reconstructions of labeled cell bodies resulting from injections in the opposite area 3a from cases 96-11 (b) and 96-9 (c and d) are also illustrated. The hindlimb representation in the opposite hemisphere was injected in (b) and (d), and the forelimb representation was injection in (c). As with case 00-16 (a), labeled cell bodies were most dense in the homotopic representation in area 3a. Labeled cell bodies were also observed in M1 and SMA. Light label was observed in areas 3b, 1 and 2, and areas S2 and PV were labeled inconsistently. Conventions as in previous figures.

other case in which the forelimb representation was injected in area 3a, similar patterns of contralateral connections were observed. However, additional label was also observed in 3b and PV, and a few labeled cells were observed in areas 1, 2, PP and S2 (Fig. 10a).

The input to the hindlimb/trunk representations in area 3a was from the expected location of the hindlimb and trunk representations in area 3a in the contralateral hemisphere (Fig. 10b,c). As with the injection in the forelimb and hand representations in area 3a, contralateral connections were also observed with M1 and SMA. A few labeled cells were also observed in areas 1, 2, 3b, PP and S2.

Cortical Architecture

The cortical myeloarchitecture was examined in tangentially sectioned cortex stained for myelin (Fig. 11a,b). The entire series of sections through the flattened cortex was reconstructed and matched with electrophysiological recording results and areal patterns of connections (see Materials and Methods). Many cortical areas were distinctly visible in a flattened section stained for myelin (Fig. 11a). For example, darkly myelinated area 3b, and extrastriate visual area MT (middle temporal area), and primary auditory cortex (A1) could be easily observed in this preparation. Some areas could be seen due to their distinct lack of myelination, such as area 3a (Fig. 11a,b). Area 3a was a thin, lightly to moderately myelinated strip of cortex that resided between the more densely myelinated M1 rostrally, and area 3b caudally (Fig. 11b). These myeloarchitectonic boundaries closely correlated with the electrophysiological determined boundaries described above.

The cytoarchitecture was also examined in parasagittally sectioned cortex stained for Nissl. In Nissl stained tissue (Fig. 11c), area 3a contained a thin granular layer (layer IV), and a prominent layer V with pronounced pyramidal cells. This differed from area 3b in which a very dense, thick granular layer is present, and layer V is attenuated. The boundary between area 3a and M1 was also apparent. At this boundary, and progressing into M1, layer IV tapered off into agranular cortex, and the thickness and packing density of pyramidal cells in layer V increased.

Discussion

In this study, we combined multi-unit electrophysiological recording and anatomical tracing techniques with myeloarchitectonic analyses to determine the topographic organization and connections of cortical area 3a in marmoset monkeys. Our results are the first demonstration in any primate of a complete representation of deep sensory receptors in area 3a. In the following discussion, we describe previous electrophysiological studies of area 3a in primates. We then consider the variability of maps generated for area 3a and speculate on the role of area 3a in somatosensory and motor processing. Finally, we describe previous studies of connections of area 3a. Although area 3a has been examined in cats (Zarzecki *et al.*, 1978; Avendano and Verdu, 1992; Avendano *et al.*, 1992; Porter, 1991, 1992) we have restricted this discussion to the details of electrophysiological and neuroanatomical studies in primates, since the behaviors that are of interest are particularly well developed in these mammals. Cats have a highly derived forepaw that is not used in tactile exploration, reaching and grasping, as is the hand of primates. Thus, while area 3a in cats and primates may be homologous, it is unlikely to be analogous.

Electrophysiological Recording Studies In Area 3a of Monkeys

Electrophysiological studies have demonstrated that the primate somatosensory cortex includes at least nine distinct cortical areas [for reviews, see (Kaas and Pons, 1988; Krubitzer, 1996; Darian Smith *et al.*, 1996)]. Some of these areas, such as 3b, 1 and 2 are well understood, while others, such as area 3a, have been less well investigated. Area 3a is particularly interesting since both single unit electrophysiological recording studies and examination of connections have indicated that area 3a plays a role in the somatosensory-motor integration network, and the vestibular cortical system. Previous studies have shown that area 3a ultimately receives input from group Ia muscle spindle afferents, and contains neurons that respond to the stimulation of these and other deep receptors in the skin [possibly RII and SAII afferents - pacinian and ruffini, respectively (Phillips *et al.*, 1971; Schwarz *et al.*, 1973; Lucier *et al.*, 1975; Heath *et al.*, 1976; Hore *et al.*, 1976); for reviews see (Jones and Porter, 1980; Tanji and Wise, 1981)].

Single unit studies in macaque monkeys have demonstrated that area 3a neurons are involved in coding muscle stretch, movement velocity, and in postural control (Yumiya *et al.*, 1974; Tanji, 1975; Wise and Tanji, 1981). Electrophysiological and neuroanatomical studies have also shown that area 3a is involved in processing vestibular information, specifically information about head-in-space movement (Guldin *et al.*, 1992; Akbarian *et al.*, 1992, 1993). In squirrel monkeys the head and neck representation in area 3a has now been termed 3aV, for vestibular cortex, because neurons in 3aV have been found to respond vigorously to stimulation of the semi-circular canal receptors (Guldin *et al.*, 1992). Finally, in a combined optical imaging electrophysiological recording study in squirrel monkeys (Tommerdahl *et al.*, 1996) neurons in area 3a were responsive to skin heating stimuli.

A few multi-unit electrophysiological recording studies in primates have demonstrated that neurons in area 3a responded to high intensity stimulation, and the gross mediolateral organization of area 3a appeared to mirror that of 3b (Krubitzer and Kaas, 1990a, Recanzone *et al.*, 1992a,c). The current study supports and substantially extends these previous observations by describing for the first time in any primate, the detailed organization of area 3a, and the specific patterns of connections of physiologically identified body part representations in area 3a with ipsilateral and contralateral cortical fields.

Taken together, the data indicate that area 3a has a general mediolateral organization from toes to tongue, that neurons respond to stimulation of deep receptors in the skin, muscles and joints [see Jones and Porter for a review (Jones and Porter, 1980)]. Additionally, the data suggest that area 3a plays a role in proprioception, vestibulo-somato integration, and possibly nociception, and receives input from posterior parietal cortex (see below), subdivisions of which are involved in the generation of body and head centered coordinates for hand and eye coordinated reaching tasks [(Ferraina and Bianchi, 1994; Snyder *et al.*, 1997, 1998); see Andersen *et al.* for reviews (Andersen *et al.*, 1997, 2000)].

Variability in Cortical Maps

We know from previous studies that areas 3b and 1 possess precise, contiguous topographic maps of the body, save for the border between the face and the hand. On the other hand, microstimulation studies of motor cortex demonstrate that motor maps are often fractured, and single movements are

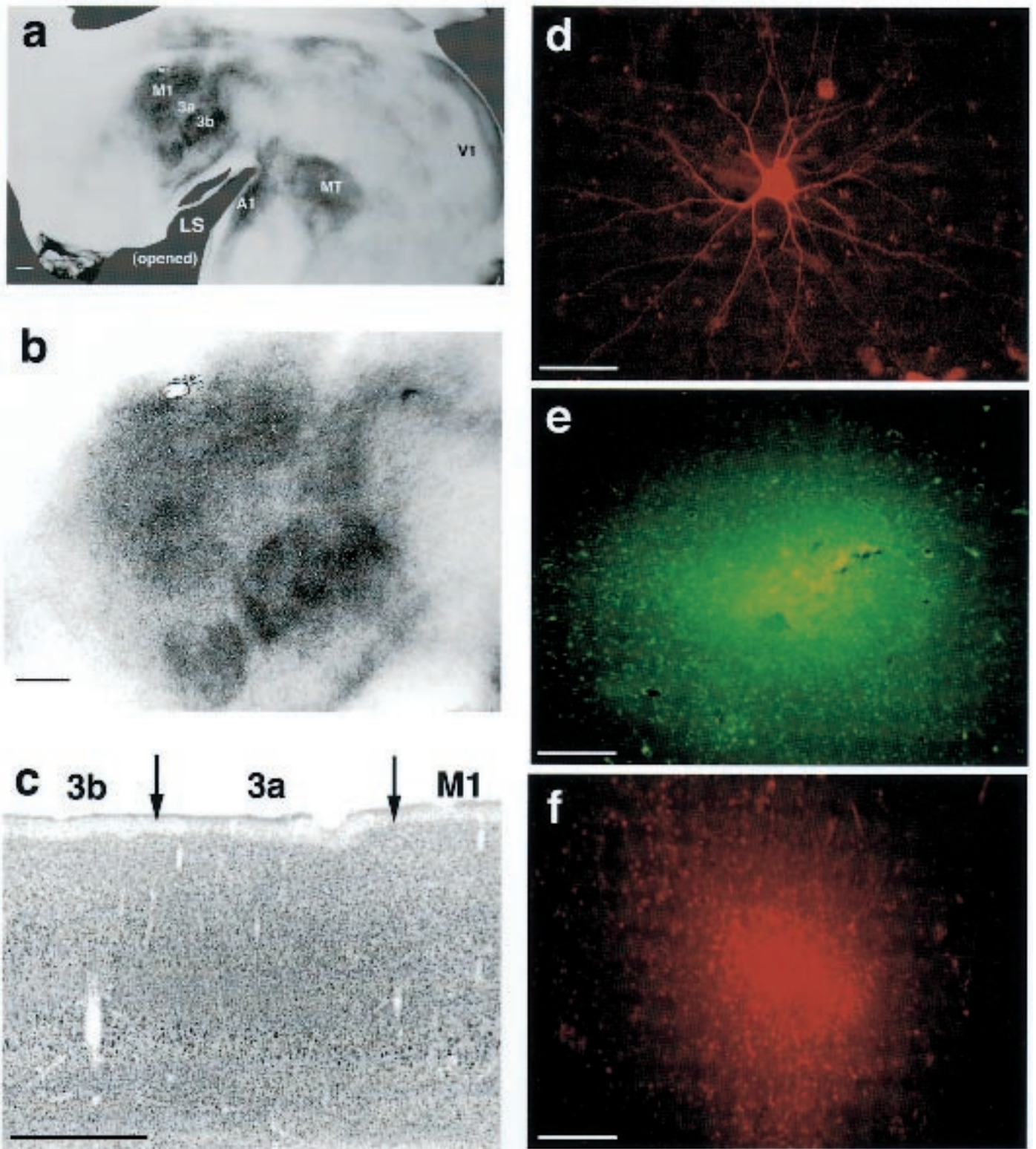


Figure 11. (a) A digital image of a flattened section of a left hemisphere, stained for myelin from case 96-11 (see Fig. 12). The lateral sulcus (LS) has been opened, and the medial wall retracted. Primary fields, such as areas 3b, M1, V1 and A1 can be distinguished in the section, and are labeled on the image. Other fields, such as areas 3a and MT can also be seen easily. Scale bar = 1 mm. Medial is up and rostral is to the left. (b) A high magnification digital image of (a) depicting M1, area 3a and area 3b, in a flattened section stained for myelin. M1 is the darkly myelinated area on the left, area 3b is the darkly myelinated area on the right, and area 3a is the light–moderately myelinated region in between. Scale bar = 1 mm. Medial is up and rostral is to the left. (c) A digital image of a parasagittal section, showing area 3a and surrounding cortex, stained for Nissl. Area 3a is the region where the granular layer IV overlaps the prominent pyramidal cells in layer V. Medial is up, rostral is to the right, scale = 1 mm. (d) A digital image of a cell labeled with FR, resulting from an injection into the forelimb representation of area 3a. This cell was located in areas 1 and 2 of the left hemisphere of case 96-9. Scale bar = 50 μm . (e) A digital image of an area 3a FE injection site in the left hemisphere of case 96-11. Scale bar = 200 μm . (f) A digital image of an area 3a FR injection site in the left hemisphere of case 96-9. Scale bar = 200 μm .

represented multiple times within an area (McGuinness *et al.*, 1980; Strick and Preston, 1982; Gould *et al.*, 1986; Nudo *et al.*, 1990; Huntley and Jones, 1991; Donoghue *et al.*, 1992; Pruess *et al.*, 1996). The current work and previous studies (Recanzone *et al.*, 1992c) demonstrate that the topographic organization of area 3a is less orderly than other somatosensory areas, and some representations in area 3a, such as the hand, are split or fractured like maps of motor cortex (see Figs 1 and 2). Further, the topographic organization of area 3a appears to be more variable between animals (Figs 1 and 2).

There are two explanations to account for these two features. The first is that there are more errors in defining the RFs for neurons in area 3a than in area 3b. Although it is more difficult to accurately define the receptive field borders for neurons representing deep receptors, the most variable representation in area 3a appeared to be the hand. In our preparation, RFs on the hand for neurons in area 3a were quite small and readily determined compared to neurons with larger RFs on the trunk. The second explanation is that there is true biological variability. We propose that the features of map organization and variability described above reflect functionally significant properties of the neurons in area 3a.

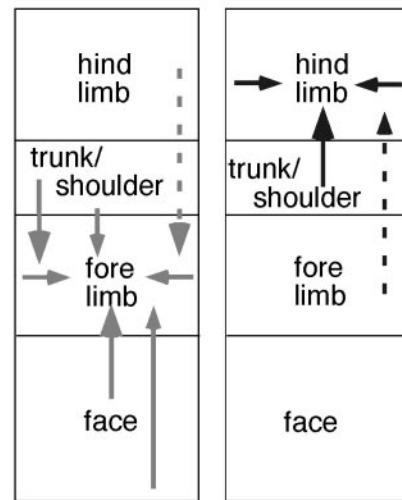
Plasticity studies in somatosensory (Merzenich *et al.*, 1983, 1984; Wall *et al.*, 1986; Calford and Tweedale, 1990), visual (Kaas *et al.*, 1990; Kaas, 2000); Darian-Smith and Gilbert, 1995; Calford *et al.*, 1999), auditory (Rajan *et al.*, 1993, Recanzone *et al.*, 1993) and motor cortex (Donoghue *et al.*, 1990, Nudo *et al.*, 1990; Sanes *et al.*, 1990; Donoghue *et al.*, 1992; Nudo *et al.*, 1996) demonstrate that changes in map organization reflect physical changes in the sensory epithelium, or alterations in the use of a particular portion of the sensory epithelium [Recanzone *et al.*, 1992a,b,c; Elbert *et al.*, 1995; Nudo *et al.*, 1996; Kleim *et al.*, 1998]; see Recanzone for a review (Recanzone 2000)]. The changes in cortical maps usually take the form of contraction or expansion of different representations of the sensory epithelium. Although extreme peripheral changes have been used to study this phenomenon, it is likely that map reconfigurations are constantly occurring normally within the life of an individual, based on use of the receptors, or changes in the use of different muscle groups in the learning of new sensory and motor tasks.

If the generation and maintenance of maps is, to a large extent, use dependent, then one might expect the greatest variability in map organization in higher order fields in which learning plays a role in their organization. For example, this study as well as other studies demonstrate that area 3a is intimately associated with motor areas involved in planning and initiation of coordinated movements [(Tanji and Kurata, 1982; Dao-fen *et al.*, 1991; Mitz *et al.*, 1991); for reviews see (Picard and Strick, 1996; Rizzolatti *et al.*, 2000)], and with posterior parietal areas involved in generating a body-centered coordinate system, hand-eye coordination and perception of extra-personal space [(Mountcastle *et al.*, 1984; Guldin *et al.*, 1992; Ferraina and Bianchi, 1994; Snyder *et al.*, 1997, 1998); see Andersen *et al.* for reviews (Andersen *et al.*, 1997, 2000)]. Finally, area 3a is also strongly connected to cingulate cortex, which is involved in learning and emotion (Lane *et al.*, 1998; Ono and Nishijo, 2000). The types of behaviors generated by these networks have a large learning component, and these behaviors are likely to change dramatically throughout life. Thus, it is not surprising that areas such as 3a, which is a key component of this network, contain more variable maps of the peripheral receptor than areas 3b and 1 (Merzenich *et al.*, 1987).

Connections of Area 3a in Primates

There are only a small number of studies in primates that have directly investigated the connections of area 3a. Much like the present investigation, area 3a in macaque monkeys has dense intrinsic input, and ipsilateral input from areas 3b (Burton and Fabri, 1995), 4 [M1 (Huerta and Pons, 1990; Stepniewska *et al.*, 1993)], SMA, 2, PP (area 5), cingulate cortex and insular cortex in the vicinity of PV and S2 (Jones *et al.*, 1978; Darian-Smith *et al.*, 1993). In the squirrel monkey, Guldin *et al.* (1992) found that area 3a had intrinsic connections and received input from areas 3b, 4 (M1), PM, 1, 2, PP (area 5), cingulate cortex, and the anterior division of area 7 (7b). An observation in the present study is the relative paucity of labeled cells in 3b after injections into electrophysiologically defined locations in 3a. This finding is supported by a previous study in macaque monkeys which also demonstrates a lack of connections with area 3b (Jones *et al.*, 1978).

a. intrinsic 3a connections



b. ipsilateral connections

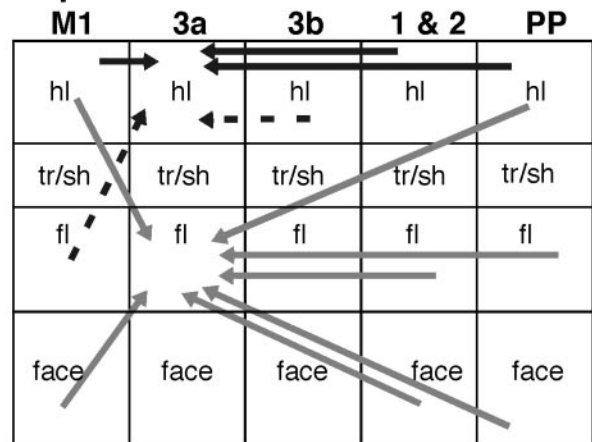


Figure 12. Schematic summary of connections. (a) The intrinsic connections of area 3a. Blue arrows on the left show input to the forelimb region, and red arrows on the right demonstrate input to the hindlimb region. Intrinsic input to the forelimb region is more widespread and from closely related and distantly related representations than input to the hindlimb region. (b) The ipsilateral input from other cortical areas to area 3a. The input to the forelimb region from other cortical areas is more widespread than the input to the hindlimb region. Solid arrows indicate dense connections and dashed arrows indicate less dense connections.

Our results expand previous studies by demonstrating that area 3a has intrinsic connections with representations that are closely related to the injection site, and with mismatched representations as well (Fig. 12). Further, intrinsic input to the hand/forearm representation in 3a appears to be more widespread than the intrinsic input to the hindlimb/trunk representation. Likewise, the labeled cells and terminals in PP, M1 and PM resulting from an injection centered in the forearm representation in area 3a appear to be more widely distributed in comparison with cells labeled from the hindlimb/trunk/shoulder injections.

Taken together, connection results indicate that a given representation within area 3a may be integrating information both within and between different body part representations, and that integration is not uniform for all body parts, but is more pronounced for behaviorally significant body part representations such as the hand and forelimb (Fig. 12). Results from the present study as well as previous studies demonstrate that area 3a plays an important role in the somatosensory-motor-vestibular integrative process (Mountcastle *et al.*, 1984; Kaas and Pons, 1988; Guldin *et al.*, 1992; Andersen *et al.*, 1997), and may contribute to the generation of an internal body-centered coordinate system, and provide information necessary for functionally relevant behaviors such as directed reaching, and hand-mouth coordination.

Notes

We wish to thank Jacopo Annesse, Elizabeth Disbrow and Gregg Recanzone for helpful comments on this manuscript, and Monika Sum for histological assistance. This work was supported by an NIH (1 RO1 NS35103-01A1) and a Whitehall Foundation (M20-97) grant to Leah Krubitzer, and by an NIMH individual National Research Service Award (1 F31 MH12284-01) to Kelly J. Huffman.

Address correspondence to Leah Krubitzer, Center for Neuroscience, 1544 Newton Ct, Davis, CA 95616, USA. Email: lakrubitzer@ucdavis.edu.

References

Aitkin L, Park V (1993) Audition and the auditory pathway of a vocal New World primate, the common marmoset. *Prog Neurobiol* 41:345-367.

Aitkin LM, Merzenich MM, Irvine DRF, Clarey JC, Nelson JE (1986) Frequency representation in auditory cortex of the common marmoset (*Callithrix jacchus jacchus*). *J Comp Neurol* 252:175-185.

Aitkin L, Kudo M, Irvine DRF (1988) Connections of the primary auditory cortex in the common marmoset (*Callithrix jacchus jacchus*). *J Comp Neurol* 269:235-248.

Akbarian S, Grusser OJ, Guldin WO (1992) Thalamic connections of the vestibular cortical fields in the squirrel monkey (*Saimiri sciureus*). *J Comp Neurol* 326:423-441.

Akbarian S, Grusser OJ, Guldin WO (1993) Corticofugal projections to the vestibular nuclei in squirrel monkeys: further evidence of multiple cortical vestibular fields. *J Comp Neurol* 332:89-104.

Andersen RA, Snyder LH, Bradley DC, Xing J (1997) Multimodal representation of space in the posterior parietal cortex and its use in planning movements. *Annu Rev Neurosci* 20:303-330.

Andersen RA, Batista AP, Snyder LH, Buneo CA, Cohen YE (2000) Programming to look and reach in the posterior parietal cortex. In: *The new cognitive neurosciences* (Gazzaniga MS, ed.), pp. 515-524. Cambridge: The MIT Press.

Avendano C, Verdu A (1992) Area 3a in the cat I. A reevaluation of its location and architecture on the basis of Nissl, myelin, acetylcholinesterase, and cytochrome oxidase staining. *J Comp Neurol* 321:357-372.

Avendano C, Isla AJ, Rausell E (1992) Area 3a in the cat II. Projections to the motor cortex and their relation to other corticocortical connections. *J Comp Neurol* 321:373-386.

Beattie J (1927) The anatomy of the common marmoset (*Hapole jacchus Kuhl*). *Proc Zool Soc Lond* 1927:593-718.

Beck PD, Kaas JH (1998) Cortical connections of the dorsomedial visual area in new world owl monkeys (*Aotus trivirgatus*) and squirrel monkeys (*Saimiri sciureus*). *J Comp Neurol* 400:18-34.

Burton H, Fabri M (1995) Ipsilateral intracortical connections of physiologically defined cutaneous representations in areas 3b and 1 of macaque monkeys: projections in the vicinity of the central sulcus. *J Comp Neurol* 355:508-538.

Calford M, Tweedale R (1990) The capacity for reorganization in adult somatosensory cortex. In: *Information processing in mammalian auditory and tactile systems* (M. Rowe, L. Aitkin, ed.), pp. 221-236. Alan R. Liss.

Calford MB, Schmid LM, Rosa MG (1999) Monocular focal retinal lesions induce short-term topographic plasticity in adult cat visual cortex. *Proc R Soc Lond Series B Biol Sci* 266:499-507.

Carlson M, Huerta MF, Cusick CG, Kaas JH (1986) Studies on the evolution of multiple somatosensory representations in primates: the organization of anterior parietal cortex in the new world Callitrichid, *Saguinus*. *J Comp Neurol* 246:409-426.

Dao-fen C, Hyland B, Maier V, Palmeri A, Wiesendanger M (1991) Comparison of neural activity in the supplementary motor area and in the primary motor cortex of monkeys. *Somatosens Mot Res* 8:27-44.

Darian-Smith C, Gilbert CD (1995) Topographic reorganization in the striate cortex of the adult cat and monkey is cortically mediated. *J Neurosci* 15:1631-1647.

Darian-Smith C, Darian-Smith I, Burman K, Ratcliffe N (1993) Ipsilateral cortical projections to areas 3a, 3b, and 4 in the macaque monkey. *J Comp Neurol* 335:200-213.

Darian-Smith I, Galea MP, Darian-Smith C (1996) Manual dexterity: how does the cerebral cortex contribute? *Clin Exp Pharm Physiol* 23: 948-956.

Donoghue JP, Suner S, Sanes JN (1990) Dynamic organization of primary motor cortex output to target muscles in adult rats. II. Rapid reorganization following motor nerve lesions. *Exp Brain Res* 79:492-503.

Donoghue JP, Leibovic S, Sanes JN (1992) Organization of the forelimb area in squirrel monkey motor cortex: representation of digit, wrist, and elbow muscles. *Exp Brain Res* 89:1-19.

Elbert T, Pantev C, Wienbruch C, Rockstroh B, Taub E (1995) Increased cortical representation of the fingers of the left hand in string players. *Science* 270:305-307.

Ferraina S, Bianchi L (1994) Posterior parietal cortex: functional properties of neurons in area 5 during an instructed-delay reaching task within different parts of space. *Exp Brain Res* 99:175-178.

Fritsches KA, Rosa MG (1996) Visuotopic organisation of striate cortex in the marmoset monkey (*Callithrix jacchus*). *J Comp Neurol* 372: 264-282.

Gallyas F (1979) Silver staining of myelin by means of physical development. *Neurology* 1:203-209.

Gould HJI, Cusick CG, Pons TP, Kaas JH (1986) The relationship of corpus callosum connections to electrical stimulation maps of motor, supplementary motor, and the frontal eye fields in owl monkeys. *J Comp Neurol* 247:297-325.

Guldin WO, Akbarian S, Grusser OJ (1992) Cortico-cortical connections and cytoarchitectonics of the primate vestibular cortex: a study in squirrel monkeys (*Saimiri sciureus*). *J Comp Neurol* 326:375-401.

Heath CJ, Hore J, Phillips CG (1976) Inputs from low threshold muscle and cutaneous afferents of hand and forearm to areas 3a and 3b of baboon's cerebral cortex. *J Physiol Lond* 257:199-227.

Hore J, Preston JB, Cheney PD (1976) Responses of cortical neurons (areas 3a and 4) to ramp stretch of hindlimb muscles in the baboon. *J Neurophysiol* 39:484-500.

Huerta MF, Pons TP (1990) Primary motor cortex receives input from area 3a in macaques. *Brain Res* 537:367-371.

Huntley GW, Jones EG (1991) Relationship of intrinsic connections to forelimb movement representations in monkey motor cortex: a correlative anatomic and physiologic study. *J Neurophysiol* 66:390-413.

Jones EG, Porter R (1980) What is area 3a? *Brain Res Rev* 2:1-43.

Jones EG, Coulter JD, Hendry SHC (1978) Intracortical connectivity of architectonic fields in the somatic sensory, motor and parietal cortex of monkeys. *J Comp Neurol* 181:291-348.

Kaas JH (1982) The segregation of function in the nervous system: why do the sensory systems have so many subdivisions? *Contrib Sens Physiol* 7:201-240.

Kaas JH (2000) The reorganization of sensory and motor maps after injury in adult mammals. In: *The new cognitive neurosciences* (Gazzaniga MS, ed.), pp. 223-236. Cambridge, MA: The MIT Press.

Kaas JH, Pons TP (1988) The somatosensory system of primates. *Comp Primate Biol* 4:421-468.

Kaas JH, Krubitzer LA, Chino YM, Langston AL, Polley EH, Blair N (1990)

- Reorganization of retinotopic cortical maps in adult mammals after lesions of the retina. *Science* 248:229-231.
- Kleim JA, Barbay S, Nudo RJ (1998) Functional reorganization of the rat motor cortex following motor skill learning. *J Neurophysiol* 80:3321-3325.
- Krubitzer L (1996) The organization of the lateral somatosensory cortex in primates and other mammals. In: Somesthesia and the neurobiology of the somatosensory cortex, International Symposium Series (Franzen O, Johanson R, Terenius L, eds), pp. 173-185, Boston, MA: Birkhaeuser.
- Krubitzer LA, Kaas JH (1990a) The organization and connections of somatosensory cortex in marmosets. *J Neurosci* 10:952-974.
- Krubitzer LA, Kaas JH (1990b) Cortical connections of MT in four species of primates: areal, modular, and retinotopic patterns. *Vis Neurosci* 5:165-204.
- Krubitzer LA, Kaas JH (1992) The somatosensory thalamus of monkeys: cortical connections and a redefinition of nuclei in marmosets. *J Comp Neurol* 319:123-140.
- Krubitzer LA, Kaas JH (1993) The dorsomedial visual area (DM) of owl monkeys: connections, myeloarchitecture, and homologies in other primates. *J Comp Neurol* 334:497-528.
- Krubitzer L, Clarey J, Tweedale R, Calford M (1998) Interhemispheric connections of somatosensory cortex in the flying fox. *J Comp Neurol* 402:538-559.
- Landgren S, Silfvenius H (1969) Projection to cerebral cortex of group I muscle afferents from the cat's hindlimb. *J Physiol* 200:353-372.
- Lane RD, Reiman EM, Axelrod B, Yun L-S, Holmes A, Schwartz G (1998) Neural correlates of levels of emotional awareness: evidence of an interaction between emotion and attention in the anterior cingulate cortex. *J Cogn Neurosci* 10:525-535.
- Lucier GE, Ruegg DC, Wiesendanger M (1975) Responses of neurons in motor cortex and in area 3a to controlled stretches of forelimb muscles in cebus monkeys. *J Physiol Lond* 251:833-853.
- Luethke LE, Krubitzer LA, Kaas JH (1989) Connections of primary auditory cortex in the New World monkey, *Saguinus*. *J Comp Neurol* 285:487-513.
- McGuinness E, Sivertsen D, Allman JM (1980) Organization of the face representation in macaque motor cortex. *J Comp Neurol* 193:591-608.
- Merzenich MM, Kaas JH, Wall J, Nelson RJ, Sur M, Felleman D (1983) Topographic reorganization of somatosensory cortical areas 3b and 1 in adult monkeys following restricted deafferentation. *Neuroscience* 8:33-55.
- Merzenich MM, Nelson RJ, Stryker MP, Cynader MS, Schoppmann A, Zook JM (1984) Somatosensory cortical map changes following digit amputation in adult monkeys. *J Comp Neurol* 224:591-605.
- Merzenich MM, Nelson RJ, Kaas JH, Stryker MP, Jenkins WM, Zook JM, Cynader MS, Schoppmann A (1987) Variability in hand surface representations in area 3b and 1 in adult owl and squirrel monkeys. *J Comp Neurol* 258:281-296.
- Mesulam M (1978) Tetramethyl benzidine for horseradish peroxidase neurohistochemistry: a non carcinogenic blue reaction-product with super sensitivity for visualizing afferents and efferents. *J Histochem Cytochem* 26:106-117.
- Mitz AR, Godschalk M, Wise SP (1991) Learning-dependent neuronal activity in the premotor cortex: activity during the acquisition of conditional motor associations. *J Neurosci* 11:1855-1872.
- Mountcastle VB, Motter BC, Steinmetz MA, Duffy CJ (1984) Looking and seeing: the visual functions of the parietal lobe. In: Dynamic aspects of neocortical function (Edelman GE, Cowan WM, Gall WE, eds), pp. 159-193. New York: John Wiley & Sons.
- Nudo RJ, Jenkins WM, Merzenich MM (1990) Repetitive microstimulation alters the cortical representation of movements in adult rats. *Somatosens Mot Res* 7:463-483.
- Nudo RJ, Milliken GW, Jenkins WM, Merzenich MM (1996) Use-dependent alterations of movement representations in primary motor cortex of adult squirrel monkeys. *J Neurosci* 16:785-807.
- Ono T, Nishijo H (2000) Neurophysiological basis of emotion in primates: neuronal responses in the monkey amygdala and anterior cingulate cortex. In: The new cognitive neurosciences (Gazzaniga MS, ed), pp. 1099-1114. Cambridge, MA: The MIT Press.
- Oscarsson O, Rosén I (1966) Short-latency projections to the cat's cerebral cortex from the skin and muscle afferents in the contralateral forelimb. *J Physiol* 182:164-184.
- Phillips CB, Powell TPS, Wiesandanger M (1971) Projections from low threshold muscle afferents of hand and forearm to area 3a of baboon's cortex. *J Physiol* 217:419-446.
- Picard N, Strick PL (1996) Motor areas of the medial wall: a review of their location and functional activation. *Cereb Cortex* 6:342-353.
- Porter L (1991) Patterns of connectivity in the cat sensory-motor cortex: a light and electron microscope analysis of the projection arising from area 3a. *J Comp Neurol* 312:404-414.
- Porter LL (1992) Patterns of projections to area 2 of the sensory cortex to area 3a and to the motor cortex in cats. *Exp Brain Res* 91:85-93.
- Preuss TM, Stepniewska I, Kaas JH (1996) Movement representation in the dorsal and ventral premotor areas of owl monkeys: a microstimulation study. *J Comp Neurol* 371:649-676.
- Rajan R, Irvine DRF, Wise LZ, Heil P (1993) Effect of unilateral partial cochlear lesions in adult cats on the representation of lesioned and unlesioned cochleas in primary auditory cortex. *J Comp Neurol* 338:17-49.
- Recanzone GH (2000) Cerebral cortical plasticity: perception and skill acquisition. In: The new cognitive neurosciences (Gazzaniga MS, ed.), pp. 237-247. Cambridge, MA: The MIT Press.
- Recanzone GH, Merzenich MM, Jenkins WM, Grajski KA, Dinse HR (1992a) Topographic reorganization of the hand representation in cortical area 3b of owl monkeys trained in a frequency discrimination task. *J Neurophysiol* 67:1031-1056.
- Recanzone GH, Merzenich MM, Schriener CE (1992b) Changes in the distributed temporal response properties of SI cortical neurons reflect improvements in performance on a temporally based tactile discrimination task. *J Neurophysiol* 67:1057-1070.
- Recanzone GH, Merzenich MM, Jenkins WM (1992c) Frequency discrimination training engaging a restricted skin surface results in an emergence of a cutaneous response zone in cortical area 3a. *J Neurophysiol* 67:1057-1070.
- Recanzone GH, Schreiner CE, Merzenich MM (1993) Plasticity in the frequency representation of primary auditory cortex following discrimination training in adult owl monkeys. *J Neurophysiol* 13:87-103.
- Rizzolatti G, Fogassi L, Gallese V (2000) Cortical mechanisms subserving object grasping and action recognition: a new view on the cortical motor functions. In: The new cognitive neurosciences (Gazzaniga MS, ed.), pp. 539-552. Cambridge, MA: The MIT Press.
- Rosa MGP, Fritsches KA, Elston GN (1997) The second visual area in the marmoset monkey: visuotopic organization, magnification factors, architectural boundaries, and modularity. *J Comp Neurol* 387:547-567.
- Sanes JN, Suner S, Donoghue JP (1990) Dynamic organization of primary motor cortex output to target muscles in adult rats. I. Long-term patterns of reorganization following motor or mixed peripheral nerve lesions. *Exp Brain Res* 79:479-491.
- Schwarz DW, Deeck L, Fredrickson JM (1973) Cortical projections of group I muscle afferents to areas 2, 3a, and the vestibular field in the rhesus monkey. *Exp Brain Res* 17:516-526.
- Snyder LH, Batista AP, Andersen RA (1997) Coding of intention in the posterior parietal cortex. *Nature* 386:167-170.
- Snyder LH, Batista AP, Andersen RA (1998) Change in motor plan, without a change in the spatial locus of attention, modulates activity in posterior parietal cortex. *J Neurophysiol* 79:2814-2819.
- Stepniewska I, Preuss TM, Kaas JH (1993) Architectonics, somatotopic organization, and ipsilateral cortical connections of the primary motor area (MI) of owl monkeys. *J Comp Neurol* 330:238-271.
- Strick PL, Preston JB (1982) Two representations of the hand in area 4 of a primate. I. Motor output organization. *J Neurophysiol* 48:139-149.
- Tanji J (1975) Activity of neurons in cortical area 3a during maintenance of steady postures by the monkey. *Brain Res* 88:549-553.
- Tanji J, Kurata K (1982) Comparison of movement-related activity in two cortical motor areas of primates. *J Neurophysiol* 48:633-653.
- Tanji J, Wise S (1981) Submodality distribution in sensorimotor cortex of the unanesthetized monkey. *J Neurophysiol* 45:467-481.
- Tommerdahl M, Delemos K, Vierck CJ, Favorov O, Whitsel B (1996) Anterior parietal cortical response to tactile and skin-heating stimuli applied to the same skin site. *J Neurophysiol* 75:2662-2670.
- Wall JT, Kaas JH, Sur M, Nelson RJ, Felleman DJ, Merzenich MM (1986) Functional reorganization in somatosensory cortical areas 3b and 1 of adult monkeys after median nerve repair: possible relationships to sensory recovery in humans. *J Neurosci* 6:218-233.

Wiesendanger M, Miles TS (1982) Ascending pathway of low-threshold muscle afferents to the cerebral cortex and its possible role in motor control. *Physiol Rev* 62:1234-1270.

Wise S, Tanji J (1981) Neuronal responses in sensorimotor cortex to ramp displacements and maintained positions imposed on hindlimb of the unanesthetized monkey. *J Neurophysiol* 45:482-500.

Yumiya H, Kubota K, Asanuma H (1974) Activities of neurons in area 3a of the cerebral cortex during voluntary movements in the monkey. *Brain Res* 78:169-177.

Zarzecki P, Shinoda Y, Asanuma H (1978) Projection from area 3a to the motor cortex by neurons activated from group I muscle afferents. *Exp Brain Res* 33:269-282.